Redox Biology 52 (2022) 102313

Contents lists available at ScienceDirect

Redox Biology

journal homepage: www.elsevier.com/locate/redox

Induction of glutathione biosynthesis by glycine-based treatment mitigates atherosclerosis

Oren Rom [a,b,c,*,1], Yuhao Liu [c,d,1], Alexandra C. Finney [a,1], Alia Ghrayeb [e,1], Ying Zhao [c], Yousef Shukha [f,g], Lu Wang [h], Krishani K. Rajanayake [h], Sandeep Das [a], Nabil A. Rashdan [i], Natan Weissman [e], Luisa Delgadillo [i], Bo Wen [h], Minerva T. Garcia-Barrio [c], Michael Aviram [g], Christopher G. Kevil [a,b,i,j], Arif Yurdagul Jr. [b,i], Christopher B. Pattillo [b,i], Jifeng Zhang [c], Duxin Sun [h], Tony Hayek [f,g], Eyal Gottlieb [e], Inbal Mor [e], Y Eugene Chen [c,**]

[a] Department of Pathology and Translational Pathobiology, Louisiana State University Health Sciences Center-Shreveport, Shreveport, LA, 71103, USA
[b] Center for Cardiovascular Diseases and Sciences, Louisiana State University Health Sciences Center-Shreveport, Shreveport, LA, 71103, USA
[c] Department of Internal Medicine, Frankel Cardiovascular Center, University of Michigan, Ann Arbor, MI, 48109, USA
[d] Department of Cardiovascular Medicine, The Second Xiangya Hospital, Central South University, Changsha, 410000, China
[e] The Laboratory for Metabolism in Health and Disease, Ruth and Bruce Rappaport Faculty of Medicine, Technion-Israel Institute of Technology, Haifa, 31096, Israel
[f] Department of Internal Medicine E, Rambam Health Care Campus, Haifa, 3109601, Israel
[g] The Lipid Research Laboratory, Ruth and Bruce Rappaport Faculty of Medicine, Technion-Israel Institute of Technology, Haifa, 3525433, Israel
[h] College of Pharmacy, Department of Pharmaceutical Sciences, University of Michigan, Ann Arbor, MI, 48109, USA
[i] Department of Molecular and Cellular Physiology, Louisiana State University Health Sciences Center-Shreveport, Shreveport, LA, 71103, USA
[j] Department of Cellular Biology and Anatomy, Louisiana State University Health Sciences Center-Shreveport, Shreveport, LA, 71103, USA

ARTICLE INFO

Keywords:
Amino acids
Atherosclerosis
Glutathione
Glycine
Macrophages

ABSTRACT

Lower circulating levels of glycine are consistently reported in association with cardiovascular disease (CVD), but the causative role and therapeutic potential of glycine in atherosclerosis, the underlying cause of most CVDs, remain to be established. Here, following the identification of reduced circulating glycine in patients with significant coronary artery disease (sCAD), we investigated a causative role of glycine in atherosclerosis by modulating glycine availability in atheroprone mice. We further evaluated the atheroprotective potential of DT-109, a recently identified glycine-based compound with dual lipid/glucose-lowering properties. Glycine deficiency enhanced, while glycine supplementation attenuated, atherosclerosis development in apolipoprotein E-deficient (*Apoe*$^{-/-}$) mice. DT-109 treatment showed the most significant atheroprotective effects and lowered atherosclerosis in the whole aortic tree and aortic sinus concomitant with reduced superoxide. In *Apoe*$^{-/-}$ mice with established atherosclerosis, DT-109 treatment significantly reduced atherosclerosis and aortic superoxide independent of lipid-lowering effects. Targeted metabolomics and kinetics studies revealed that DT-109 induces glutathione formation in mononuclear cells. In bone marrow-derived macrophages (BMDMs), glycine and DT-109 attenuated superoxide formation induced by glycine deficiency. This was abolished in BMDMs from glutamate-cysteine ligase modifier subunit-deficient (*Gclm*$^{-/-}$) mice in which glutathione biosynthesis is impaired. Metabolic flux and carbon tracing experiments revealed that glycine deficiency inhibits glutathione formation in BMDMs while glycine-based treatment induces *de novo* glutathione biosynthesis. Through a combination of studies in patients with CAD, *in vivo* studies using atherosclerotic mice and *in vitro* studies using macrophages, we demonstrated a causative role of glycine in atherosclerosis and identified glycine-based treatment as an approach to mitigate atherosclerosis through antioxidant effects mediated by induction of glutathione biosynthesis.

* Corresponding author. Department of Pathology and Translational Pathobiology, Louisiana State University Health Sciences Center-Shreveport, 1501 Kings Highway, Shreveport, LA, 71103, USA.
** Corresponding author. Department of Internal Medicine, University of Michigan, 2800 Plymouth Road, Ann Arbor, MI, 48109, USA.
E-mail addresses: oren.rom@lsuhs.edu (O. Rom), echenum@umich.edu (Y.E. Chen).
[1] Equal contribution.

https://doi.org/10.1016/j.redox.2022.102313
Received 14 March 2022; Received in revised form 4 April 2022; Accepted 8 April 2022
Available online 13 April 2022

1. Introduction

Glycine, the simplest among the 20 natural amino acids, can be synthesized endogenously and is thus classified as a nonessential amino acid. However, previous studies indicate that glycine synthesis may be insufficient to meet the organism's metabolic needs, suggesting that glycine is a conditionally essential amino acid [1–3]. Glycine has multiple biological and physiological roles and is necessary for the synthesis of essential molecules such as purines [4], heme [5], creatine [6], and glutathione [7,8]. Lower circulating levels of glycine are consistently reported in association with various cardiometabolic diseases including obesity [9], type 2 diabetes (T2D) [10], metabolic syndrome [11], non-alcoholic fatty liver disease (NAFLD) [7,8,12], acute myocardial infarction [13], and coronary heart disease [14]. We and others demonstrated that low glycine availability is a limiting factor for glutathione biosynthesis, which is restored by glycine supplementation, leading to lower oxidant damage in NAFLD and T2D [7,8,15]. While potential mechanisms by which glycine protects against NAFLD and T2D have been identified [7,8,15–18], the causative role and therapeutic potential of glycine in atherosclerosis, the underlying cause of most CVDs [19], remain to be established.

Atherosclerosis is a chronic disease of the arteries arising from imbalanced lipid metabolism, maladaptive immune response and dysregulated redox homeostasis [19–21]. Atherosclerosis develops in response to the biologic effects of underlying risk factors, including dyslipidemia, T2D, obesity and NAFLD [22,23]. Reductions in those risk factors significantly lowers the risk of cardiovascular events and death [24]. Specifically, current treatment guidelines focus on reduction of circulating cholesterol, particularly low-density lipoprotein cholesterol (LDL-C), due to its well-established role in atherosclerotic cardiovascular disease (CVD) [22,25]. However, despite remarkable advances in LDL-C-lowering drugs, numerous clinical trials of statins, non-statins, and combination therapies have shown persistent residual risk of atherosclerotic CVD [25], which remains a leading cause of death worldwide [22]. This is likely due to lack of influence or detrimental effects of current cholesterol-lowering therapies on cardiometabolic risk factors beyond LDL-C [26]. For instance, while markedly lowering LDL-C, statin therapy enhances the risk of new-onset T2D, increases body weight, and has no clear benefit in NAFLD [27,28]. Therefore, identification of new metabolic pathways that can be targeted for the treatment of atherosclerosis without increasing, and preferably while decreasing, other cardiometabolic risk factors, is of great significance in the effort to reduce CVD burden [26]. Considering consistent reports linking lower circulating glycine with various cardiometabolic diseases and its protective effects in NAFLD and T2D [9–18], there is strong rationale to evaluate the causative role and therapeutic potential of glycine in atherosclerosis.

In line with epidemiological evidence linking higher circulating glycine levels with a favorable lipid profile [13], we and others demonstrated that dietary and genetic approaches to limit glycine availability increase, while glycine supplementation decreases, hyperlipidemia and lipid accumulation [8,17,29–32]. Although those previous reports suggest a potential atheroprotective role of glycine, its direct effect on atherosclerosis remain unknown. Furthermore, it is unclear whether the potential atheroprotective effects of glycine are mediated through lipid-lowering effects or other underlying mechanisms. Here, motivated by the identification of reduced circulating glycine in patients with significant coronary artery disease (sCAD), we studied a causative role of glycine in atherosclerosis and evaluated the atheroprotective potential of DT-109, a recently identified glycine-based compound that ameliorates NAFLD [8]. Utilizing dietary approaches to manipulate glycine availability in apolipoprotein E-deficient (*Apoe*$^{-/-}$) mice combined with metabolic flux studies in isolated macrophages, we demonstrated a causative role of glycine in atherosclerosis and identified a glycine-based treatment to mitigate atherosclerosis through antioxidant effects mediated by induction of *de novo* glutathione biosynthesis, independent of lipid-lowering effects.

2. Materials and methods

2.1. Clinical study

The study included patients that presented with acute chest pain suspected to be of cardiac origin, as we recently described [30]. The patients were admitted to the chest pain unit in the Department of Internal Medicine E, Rambam Health Care Campus, Haifa, Israel. The study was approved by the local Institutional Review Board (protocol 0373-18-RMB, Clinical Trial Registration: NCT03646019). All participants gave informed consent. Exclusion criteria included a prior diagnosis of CAD, allergy to iodine contrast agents, contraindication for radiations, asthma exacerbation, current use of steroids or other immunomodulating drugs, renal insufficiency (creatinine level $\geq$1.5 mg/dl), fever during the last 48 h prior to admission, concomitant inflammatory diseases (infections, autoimmune disorders, kidney and liver diseases, and recent major surgical procedure), valvular, myocardial or pericardial diseases and poor quality of computed tomography (CT) image due to motion artifacts or inappropriate contrast delivery resulting in non-diagnostic image quality. Ninety-five patients met the above criteria and underwent coronary computed tomography angiography (CCTA) to assess atherosclerosis in their coronary arteries. The patients were divided in groups with sCAD (coronary artery stenosis >49%, n = 24) or without sCAD (coronary artery stenosis $\leq$49%, n = 71). Calcium scoring was determined by the Agatston method [33]. Blood samples were obtained following a 10 h overnight fast. Serum biochemical analyses were performed by technicians blinded to the groups. Demographics, drug use and biochemical parameters of patients with or without sCAD are detailed in Supplemental Table 1. To control for potential confounding factors, we applied case-control matching and randomization (IBM SPSS software version 23.0). Twenty-four age-, sex-, and blood pressure-matched patients that were found to have no sCAD were randomly assigned as controls.

2.2. Animal studies

Animal procedures were approved by the Institutional Animal Care & Use Committees of the University of Michigan (PRO00008239) and Louisiana State University Health Sciences Center-Shreveport, Shreveport (P-21-043). All studies were performed in accordance with the institutional guidelines. *Apoe*$^{-/-}$ mice (B6.129P2-Apoe$^{tm1Unc/J}$, stock: 002052) and C57BL/6J (stock: 000664) were purchased from Jackson Laboratories. Glutamate-cysteine ligase modifier subunit-deficient (*Gclm*$^{-/-}$) mice, a gift from Dr. Terrance Kavanagh [34,35], were bred and housed at the Animal Resource Facility of Louisiana State University Health Sciences Center-Shreveport. For atherosclerosis studies, eight-week-old male *Apoe*$^{-/-}$ mice were fed ad libitum either an amino acid (AA)-defined Western diet (Envigo-Teklad, 42% fat, 0.2% cholesterol) with glycine (WD_{AA} + Gly, TD.170525) or without glycine (WD_{AA} -Gly, TD.170526), as we previously described [8], a standard Western diet (WD, Envigo-Teklad TD.88137, 42% fat, 0.2% cholesterol) or a low-fat standard diet (SD, LabDiet 5L0D, 13% fat). Eight-week old male C57BL/6J mice were used for glutathione kinetics studies. When indicated, mice were orally administered (gavage) glycine, leucine (Sigma-Aldrich G5417 and L8912, respectively) or DT-109 (Beijing SL Pharmaceutical) at 0.17–1 mg/g body weight per day or H_2O as control, as we previously described [8]. Bone marrow derived macrophages (BMDMs) were isolated from C57BL/6J and *Gclm*$^{-/-}$ mice as described below.

2.3. Targeted metabolomics and plasma analyses

Circulating glycine levels were measured in serum samples from patients with and without sCAD by investigators blinded to the study

groups as we previously described [8,30]. Briefly, liquid chromatography (LC)-mass spectrometry (MS)/MS was used to measure serum amino acids using isotope-labeled amino acids (MSK-CAA-1, Cambridge Isotopes Laboratory) as internal standard. The LC-MS/MS analysis was performed using a Shimadzu LC-20AD HPLC system (Shimadzu Corporation) coupled in-line to an AB Sciex QTrap 5500 system (Applied Biosystems) equipped with an electrospray ionization source. Chromatographic separation was conducted on an Agilent Poroshell 120 EC-C18 column (50 mm × 2.1 mm I.D., 2.7 μm; Agilent) at a flow rate of 0.4 mL/min. The mobile phase consisted of water (A) and acetonitrile containing 0.1% (v/v) formic acid (B). The mass spectrometer was operated in positive ionization mode with multiple reaction monitoring (MRM). Analyst version 1.6.2 software (Applied Biosystems) was used for data acquisition and analysis. In mice, blood glucose levels were measured using glucometer and test strips (Contour Next). Plasma samples were analyzed for total cholesterol (TC) and triglycerides (TG) using the Wako Cholesterol E kit (999-02601, FUJIFILM medical system) and LabAssay Triglyceride kit (290-63701, FUJIFILM medical system).

2.4. Analysis of atherosclerosis in mice

Analyses of atherosclerosis in the aortic sinus and whole aortic tree were performed as we previously described [30,36]. All analyses were conducted in accordance with the American Heart Association recommendations for experimental atherosclerosis studies [37]. For analysis of atherosclerosis in the aortic sinus, formalin-fixed samples were cryoprotected in 20% sucrose at 4 °C overnight, blotted, then liquid nitrogen-snap frozen in O.C.T. Compound (Tissue-Tek) and stored at −80 °C until cryo-sectioning. Prior to sectioning, frozen blocks were brought up to approximately −20 °C, then sectioned at 5 μm on a Leica Cryostat (CM3050S). Slides were stored at −80 °C until stained. Prior to staining, the slides were thawed to room temperature for 30 min and then stained for H&E staining with Harris hematoxylin (ThermoFisher Scientific), rinsed in tap water and treated with Clarifier (ThermoFisher Scientific). Slides were then rinsed in tap water and the nuclei were counter stained with bluing reagent (ThermoFisher Scientific), rinsed in 70% ethanol, stained with eosin Y, alcoholic (ThermoFisher Scientific), then dehydrated and cleared through graded alcohols and xylene and mounted with Micromount (Leica 3801731) using a Leica CV5030 automatic coverslipper. For dihydroethidium (DHE) immunofluorescence, slides were rinsed for 2 min with PBS (x3) and then stained with 5 μM DHE (Sigma-Aldrich D7008) at 37 °C for 30 min in the dark. After washing with PBS (x3), the slides were mounted with ProLong™ Gold Antifade Mountant with DAPI (Invitrogen P36935), and images were captured using an Olympus DP73 microscope. The atherosclerotic plaque area and DHE fluorescence at the three valve leaflets were quantified using ImageJ software (NIH). En face atherosclerosis was performed as we previously described [30,36]. The entire length of the aorta from the heart to the iliac bifurcation was removed. After clearing the adventitial tissue, aortas were stained with oil red O (ORO), opened longitudinally and pinned flat onto a dark wax plate. The percentage of ORO positive area was calculated using ImageJ (National Institutes of Health, NIFH).

2.5. Analysis of glutathione in tissues

Eight-week-old male C57BL/6J mice were orally administered DT-109 (0.5 mg/g). Mouse blood mononuclear cells were isolated at baseline, before DT-109 administration (0 h), and after 2, 6 and 24 h using Ficoll-Paque PREMIUM 1.084 (Sigma-Aldrich GE17-5446-02) in accordance with the manufacturer's instructions. Briefly, heparinized blood samples were diluted with equal volume of DPBS and carefully combined with the Ficoll-Paque media solution in a 15-mL centrifuge tube. The tubes were centrifuged at 400 g for 30 min (20 °C). The mononuclear cell layer was collected and washed twice with DPBS to remove residual plasma. To quantitate reduced glutathione (GSH) and oxidized glutathione (GSSG), mononuclear cells were lysed via ultrasound and diluted 1:20 in PBS. 180 μL of methanol containing 25 nM internal standard was added to 50 μL of diluted samples. The mixture was vortexed for 10 min for protein precipitation. The extracts were centrifuged at 3,500 rpm for 10 min, and 200 μL of supernatant was transferred to a 96-well plate. The supernatant was evaporated using a vacuum concentrator (SpeedVac DNA 130) for 4 h at 35 °C. The dry extracts were reconstituted in 80 μL water, vortexed for 10 min and centrifuged at 3,500 rpm for 10 min at 4 °C. Supernatants were then transferred to autosampler vials for LC-MS/MS analysis. Mouse hearts and aortas were isolated at baseline, before DT-109 administration (0 h), and after 2, 6, and 24 h. An aliquot of 50 μL of tissue samples were added to a 100 μL aliquot of acetonitrile containing 50 nM CE 302 and 50 μL of acetonitrile. The mixture was vortex-mixed for 10 min and centrifuged at 3,500 rpm for 10 min at 4 °C. A 10 μL aliquot of the resulting supernatant was injected into the LC-MS/MS system for analysis. The analytical curve for GSH and GSSG quantification was constructed with 10 nonzero standards by plotting the peak area ratio of analyte to the internal standard versus the sample concentration, using PBS as a solvent. The concentration ranges from 1 to 1000 ng/mL. A blank sample (matrix sample processed without internal standard) was used to exclude contamination or interference.

2.6. Bone marrow derived macrophages (BMDMs)

BMDMs were obtained as we previously described [30,38], with minor modifications. Briefly, bone marrow was flushed from the femurs and tibias of 8–10-week-old C57BL/6J, *Gclm*$^{+/+}$ and *Gclm*$^{-/-}$ mice using PBS and a 26G needle. Cells were filtered through a 70 μm cell strainer and plated onto 10 cm petri dishes. Cells were maintained in growth medium containing Dulbecco's Modified Eagle's Medium (DMEM, Genesee #25-501), 20% FBS (Gibco), 1% penicillin/streptomycin (Genesee #25-512), 1 mM sodium pyruvate (Corning #25-000-C1), and 5 ng/mL murine m-CSF (Peprotech 315-02-50UG). After 3-4 days the media was completely replaced with fresh growth media. Adherent macrophages were lifted from the plate using 10 mM ETDA in PBS and scraping and seeded in cell culture plates for experiments.

2.7. Protein extraction and Western blot

Immunoblotting was performed as we previously described [39]. For protein analysis, BMDMs were plated onto 6-well plates at 1 × 10^6 cells per well. Cells were lysed in 2× Laemmli buffer (Bio-Rad #1610737) and heat-denatured at 95 °C for 10 min. Lysates were normalized to total protein using Pierce 660 Protein Assay reagent (Thermo Fisher #22660) and alpha-cyclodextrin (Fisher #C077610G) and adjusted for equal protein loading. Samples were separated by gel electrophoresis using 10% TGX Stain-Free FastCast Acrylamide gels (Bio-Rad #1610182) and transferred to nitrocellulose membranes (Bio-Rad #1704158). Membranes were incubated overnight with either rabbit anti-GCLM (1:1000, Proteintech #14241-1-AP) or mouse anti-GAPDH antibody (1:5000, Santa Cruz Biotechnology #sc-365062). Primary antibodies were labeled with IRDye-conjugated secondary antibodies (1:10,000, LI-COR Biosciences #926-32212 or #926-68073). Secondary antibodies were visualized with an Odyssey Fc Imaging System (LI-COR Biosciences) and analyzed using LI-COR Imaging Studio Software version 1.0.37.

2.8. Superoxide analysis

BMDMs were plated onto either 8-well chamber slides (Thermo Fisher #177402 PK) at 1.5 × 10^5 cells per well or glass-bottom 96 well plates (Cellvis #P96-0-N) at 4 × 10^4 per well. Cells were allowed to adhere overnight in growth medium, then media was replaced with metabolic medium containing Earl's Balanced Salt Solution (EBSS, Gibco #24010-043), 1× MEM amino acids solution (Gibco #11140-

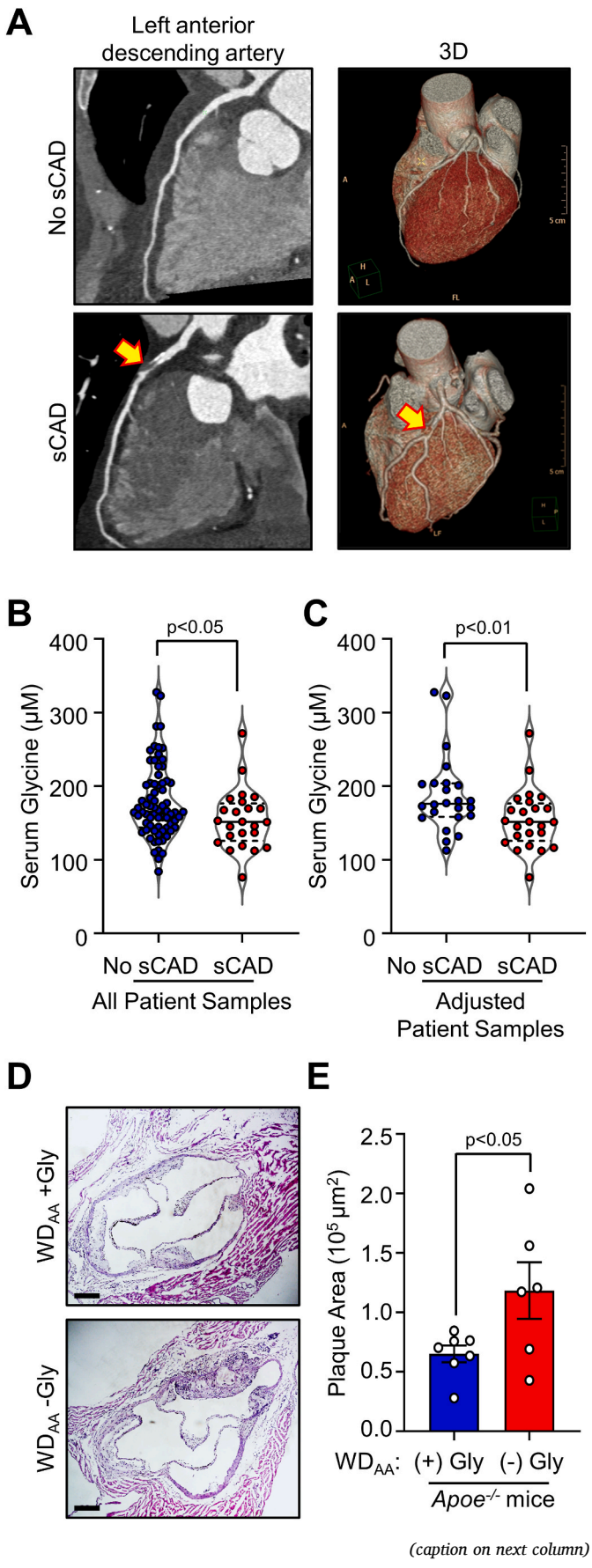

(caption on next column)

Fig. 1. Circulating glycine is decreased in patients with significant coronary artery disease and glycine deprivation enhances atherosclerosis in *Apoe*$^{-/-}$ mice. (A) Patients with acute chest pain suspected to be of cardiac origin underwent coronary computed tomography angiography (CCTA) to assess atherosclerosis in the coronary arteries (n = 95). Twenty-four patients were found to have significant coronary artery disease (sCAD) and 71 patients were found to have no sCAD. Representative CCTA with curved multiplanner reconstruction and 3D volume rendering from patients with and without sCAD are shown. Significant coronary artery stenosis is indicated by yellow arrows. Serum glycine concentrations were analyzed by LC-MS/MS **(B)** in all patients, and **(C)** in 24 age-, sex-, and blood pressure-matched patients with or without sCAD. **(D–E)** *Apoe*$^{-/-}$ mice were fed an amino acid-defined Western diet with glycine (WD_{AA} + Gly) or without glycine (WD_{AA} -Gly) for 10 weeks. Atherosclerotic plaque area in the aortic sinus was analyzed (n = 6–7, scale bar: 200 μm). Data are presented as violin plots or as mean ± SEM showing all points. Statistical differences were compared using unpaired *t*-test or Mann-Whitney U *t*-test.

050), 1× MEM vitamins solution (Fisher #11-120-052), 0.25 mM L-Serine (Fisher #AAA1117914), 1 mg/L glutathione (Fisher #ICN10181405), 0.3 ng/mL ammonium metavanadate (Fisher #AC194910500), 0.25 nM manganese chloride (Sigma #M3634), 2.5 μg/mL L-ascorbic acid (Fisher #AAA1561318), 1× ITS liquid media supplement (Sigma #I3146), and 2.5% heat-inactivated FBS (Gibco). Metabolic media was either supplemented with water control (glycine-depleted), 1 mM glycine, or 1 mM DT-109 [8]. BMDMs were maintained in metabolic medium with supplements for 18 h. Cells were then rinsed 3 times with warmed HBSS (Fisher #21-021-CV) and DHE was added at 5 μM for 30 min at 37 °C. Nuclei were stained with Hoechst (1:20,000 dilution, Fisher #0062249) during this time. After rinsing 3 times with warmed HBSS, the cells were visualized using a Keyence BZ-X800 fluorescence microscope and analyzed with the Keyence BZ-X800 Analyzer software version 1.1.2.4. During imaging, cells were maintained at 37 °C and 5% CO_2 with a Tokai Hit Stage Top Incubator. DHE fluorescence was normalized to total number of Hoechst per high powered field. At least 3 images per treatment were taken.

2.9. Metabolic flux and carbon tracing

BMDMs were incubated in glycine-deprived metabolic medium as described above. After 24 h, the medium was replaced with fresh metabolic medium enriched with 1 mM U–$^{13}C_5$ labeled glutamine (Cambridge Isotope Laboratories Inc.) for 5 h in the presence or absence of 1 mM glycine or 1 mM DT-109. Metabolite extraction from the cells and LC-MS analysis were performed as we previously described [8]. TraceFinder™ 4.1 (ThermoFisher Scientific) was used for analysis. Peak areas of metabolites were determined using the exact mass of the singly charged ions. The retention time of metabolites was predetermined on the pHILIC column (Merck) by analyzing an in-house mass spectrometry metabolite library consisting of commercially available standards. For data normalization, raw data files were processed with Compound Discoverer 3.0 (ThermoFisher Scientific) to obtain total compound's peak area for each sample. Metabolite peak area was normalized to total measurable ions in the sample. Data ware visualized using Metabolite Autoplotter as we previously described [8].

2.10. RNA preparation and RT-qPCR analysis

Total RNA from mouse liver samples was extracted using Trizol reagent (ThermoFisher Scientific 15596026) and purified with QIAGEN's RNeasy kit (QIAGEN 74106) as we previously described [8,30]. RNA was reverse-transcribed into cDNA with SuperScript III and random primers (Thermo Fisher Scientific 18080051). Specific transcript levels were assessed by a real-time PCR system (Bio-Rad CFX96) using iQ SYBR Green Supermix (Bio-Rad 1708882) and the ΔΔCt threshold cycle method of normalization. Gene expression levels were normalized to

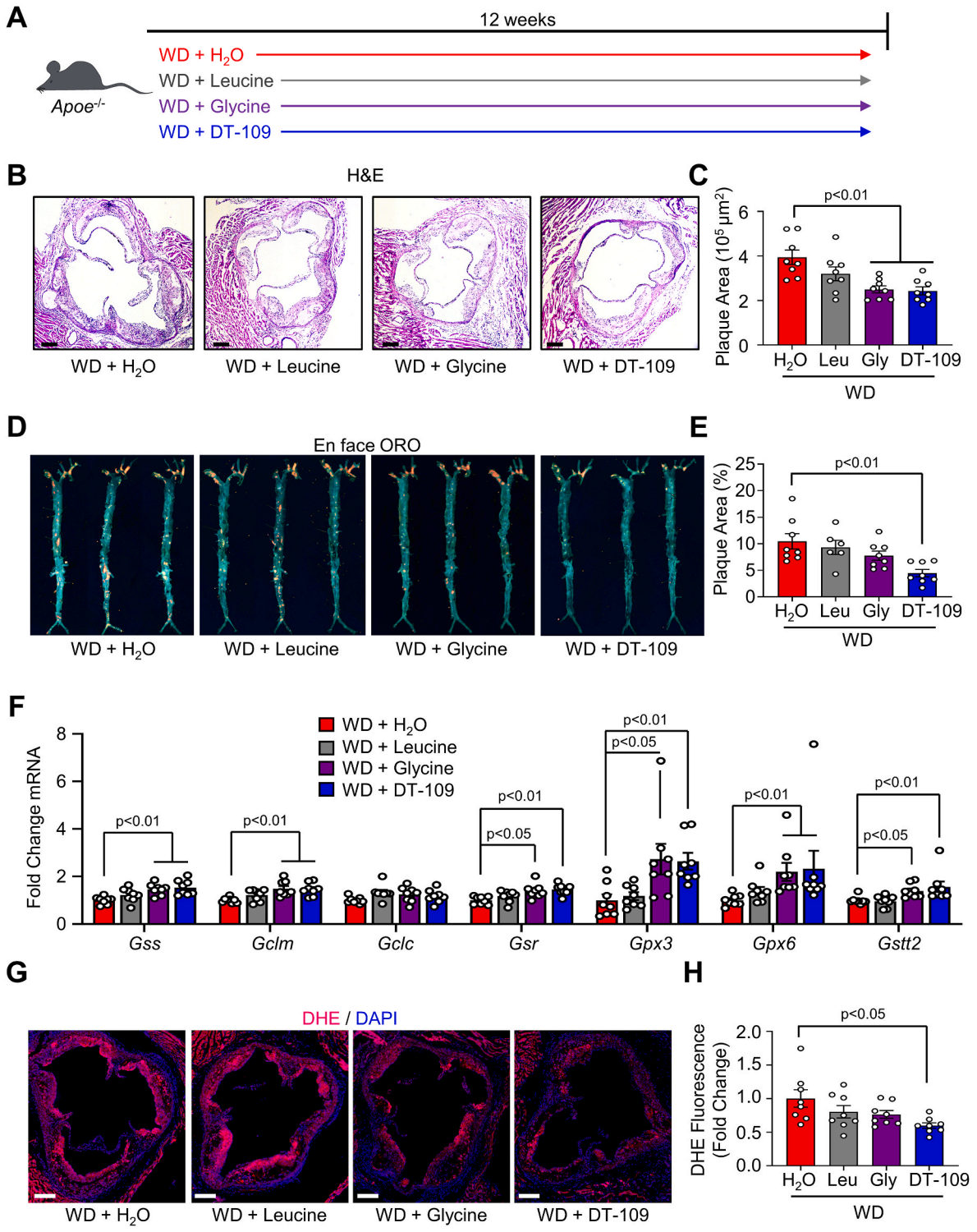

Fig. 2. Glycine-based treatment reduces atherosclerotic plaque size and superoxide. (A) *Apoe*$^{-/-}$ mice were fed a Western diet (WD) for 12 weeks and orally administered water supplemented with DT-109 (1 mg/g body weight/day) or equivalent levels of leucine (Leu, 0.33 mg/g body weight/day), glycine (Gly, 0.66 mg/g body weight/day) or water control (H_2O). **(B–C)** Atherosclerotic plaques in the aortic sinus were analyzed for plaque area using H&E (n = 8, scale bar: 200 µm). **(D–E)** Whole aortas were stained en face with oil red O (ORO) and plaque area was expressed as a percentage of the total aorta area (n = 6–8). **(F)** Livers were collected at endpoint and analyzed for glutathione metabolic genes. Expression of *Gss* (glutathione synthetase), *Gclm/c* (glutamate-cysteine ligase modifier and catalytic subunits, respectively), *Gsr* (glutathione disulfide reductase), *Gpx3/6* (glutathione peroxidase 3 and 6, respectively), and *Gstt2* (glutathione S-transferase theta 2) was normalized to *Gapdh* and expressed as fold change from WD with water (H_2O) treatment (n = 8). **(G–H)** Aortic sinuses were analyzed for superoxide using dihydroethidieum (DHE, red) with a nuclear counterstain (DAPI, blue). DHE fluorescence for each treatment was expressed as fold change from WD with H_2O treatment (n = 8, scale bar: 200 µm). Data are presented as mean ± SEM showing all points. Statistical differences were compared using one-way ANOVA with Tukey's post hoc analysis or Kruskal-Wallis test followed by Dunn's post-hoc analysis. (For interpretation of the references to colour in this figure legend, the reader is referred to the Web version of this article.)

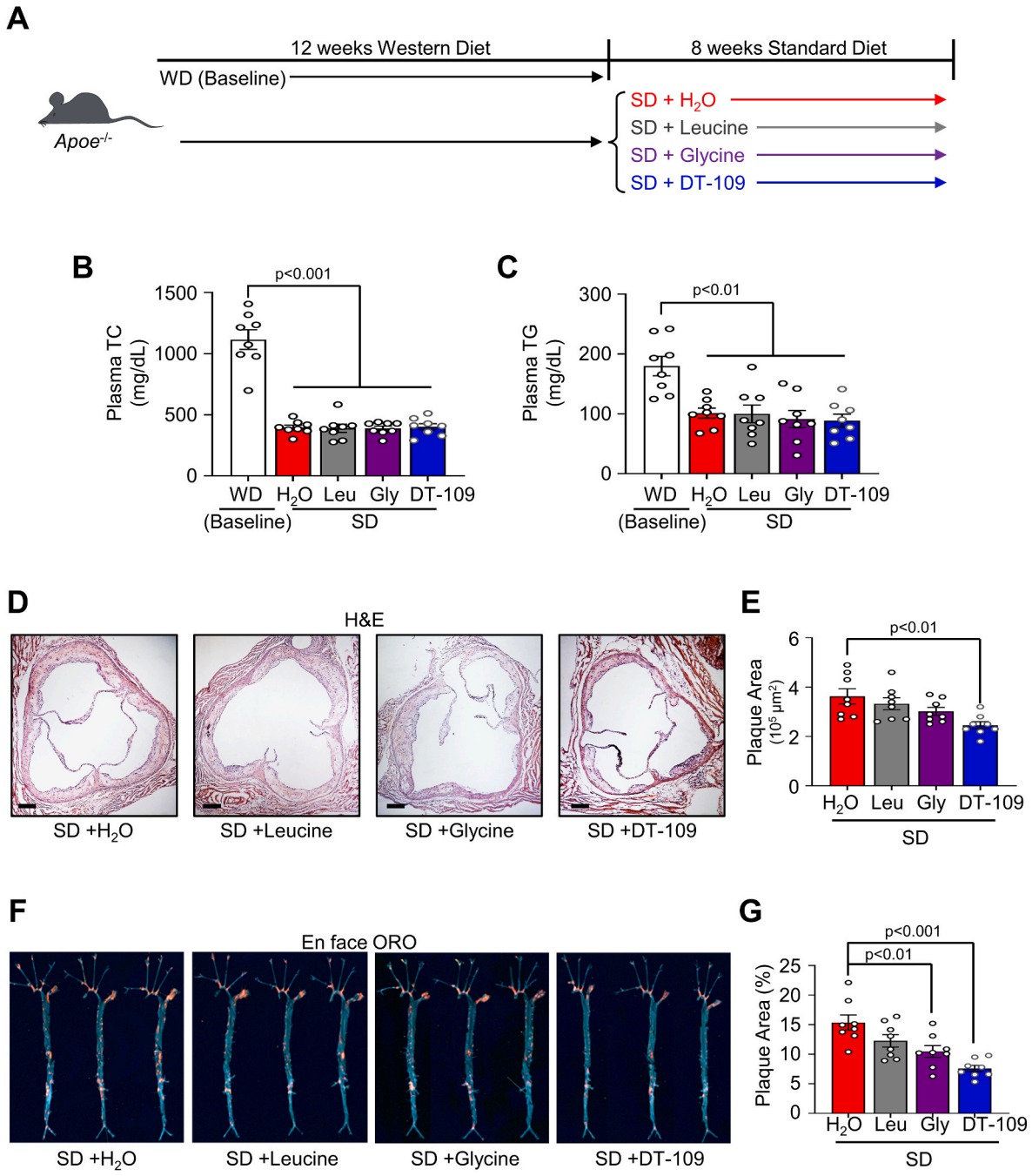

Fig. 3. Glycine-based intervention reduces atherosclerosis independent of lipid-lowering effects. (A) *Apoe*$^{-/-}$ mice were fed a Western diet for 12 weeks to develop atherosclerosis (baseline), then placed onto standard diet (SD) for additional 8 weeks with oral administration of water supplemented with DT-109 (0.5 mg/g body weight/day) or equivalent levels of leucine (Leu, 0.17 mg/g body weight/day), glycine (Gly, 0.33 mg/g body weight/day) or water control (H_2O). **(B)** Plasma total cholesterol (TC), and **(C)** plasma triglycerides (TG) at endpoint (n = 8). **(D–E)** Atherosclerotic plaques in the aortic sinus were analyzed for plaque area using H&E (n = 8, scale bar: 200 µm). **(F–G)** Whole aortas were stained en face with oil red O (ORO) and plaque area was expressed as a percentage of the total aorta area (n = 8). Data are presented as mean ± SEM showing all points. Statistical differences were compared using one-way ANOVA with Tukey's post hoc analysis. (For interpretation of the references to colour in this figure legend, the reader is referred to the Web version of this article.)

glyceraldehyde 3-phosphate dehydrogenase (*Gapdh*). Primer pairs used for RT-qPCR were obtained from Integrated DNA Technologies and are listed in Supplemental Table 2.

2.11. Statistical analyses

Statistical analyses were performed using GraphPad Prism version 8.0. For the clinical study, case-control matching and randomization was performed using IBM SPSS software version 23.0. All data were tested for normality using the Shapiro-Wilk test. If passed, Student's *t*-test was used to compare two groups and one-way ANOVA followed by Tukey post-hoc test for comparisons among >2 groups. Otherwise, nonparametric tests (Mann-Whitney *U* test or Kruskal-Wallis test followed by Dunn's post-hoc test) were used. Differences between categorical variables were tested using Fisher's exact test. Data are presented as mean ± SEM and $p < 0.05$ was considered statistically significant.

3. Results

3.1. Circulating glycine is decreased in patients with significant coronary artery disease and glycine deprivation enhances atherosclerosis in mice

To determine whether circulating glycine levels are altered in patients with atherosclerosis, we used LC-MS/MS to measure glycine concentrations in serum samples from patients with significant coronary artery disease (sCAD) compared to those with no sCAD. Among 95 patients that met the inclusion and exclusion criteria of the clinical study and underwent CCTA to assess atherosclerosis in their coronary arteries (Fig. 1A), 24 patients were found to have sCAD. As detailed in Supplemental Table 1, patients with sCAD had a significantly higher calcium score ($p<0.0001$), a well-established feature of coronary atherosclerosis [33], were significantly older ($p = 0.0193$), included more males ($p = 0.0228$), and showed a trend toward increased systolic blood pressure

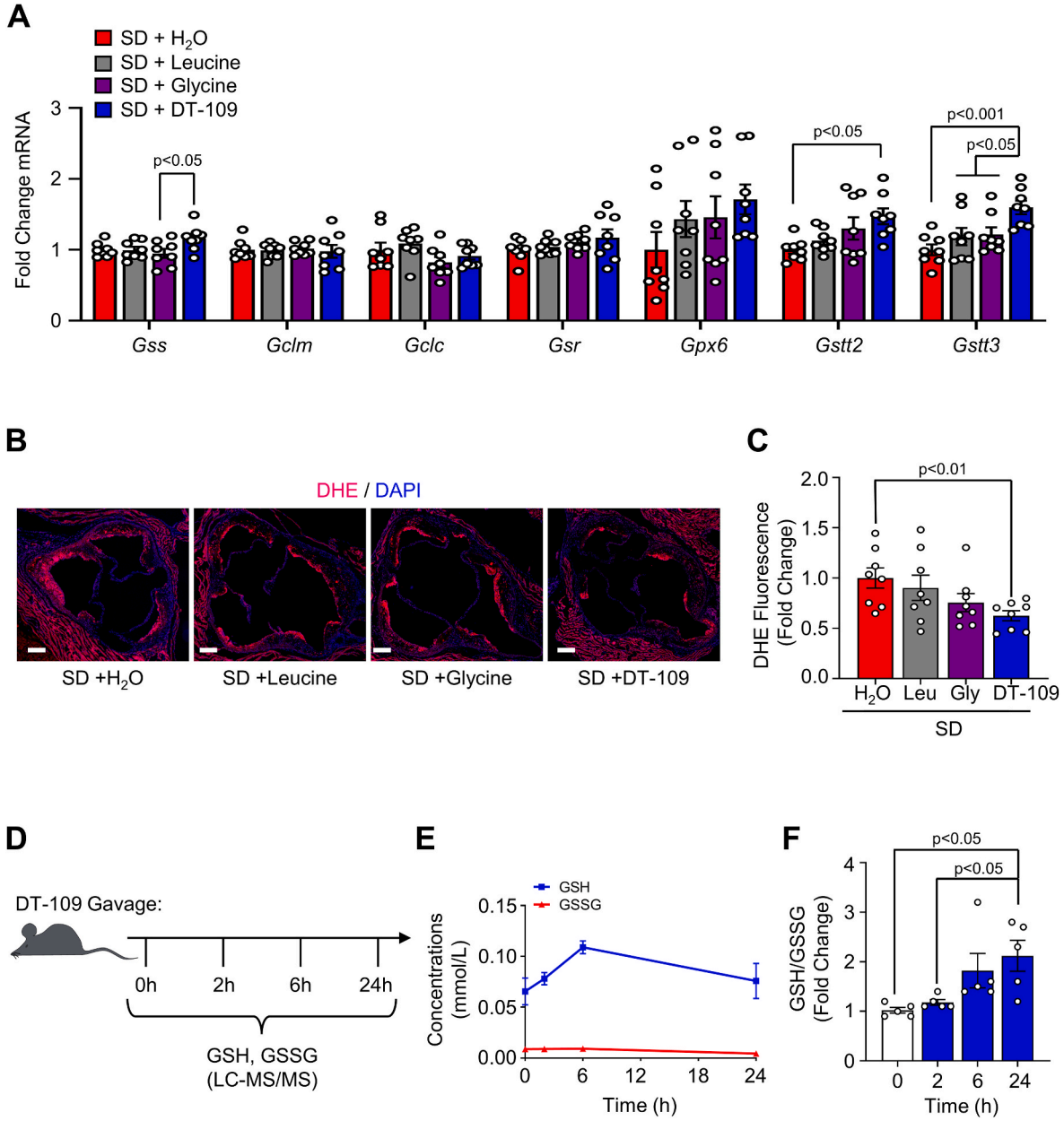

Fig. 4. Glycine-based intervention reduces plaque superoxide and enhances GSH formation in mononuclear cells. *Apoe*$^{-/-}$ mice were fed a Western diet for 12 weeks to develop atherosclerosis (baseline), then placed onto standard diet (SD) for additional 8 weeks with oral administration of water supplemented with DT-109 (0.5 mg/g body weight/day) or equivalent levels of leucine (Leu, 0.17 mg/g body weight/day), glycine (Gly, 0.33 mg/g body weight/day) or water control (H_2O). **(A)** Livers were collected at endpoint and analyzed for glutathione metabolic genes. Expression of *Gss* (glutathione synthetase), *Gclm/c* (glutamate-cysteine ligase modifier and catalytic subunits, respectively), *Gsr* (glutathione disulfide reductase), *Gpx6* (glutathione peroxidase 6), and *Gstt2/3* (glutathione S-transferase theta 2 and 3, respectively) was normalized to *Gapdh* and expressed as fold change from SD with water (H_2O) treatment (n = 8). **(B–C)** Aortic sinuses were analyzed for superoxide using dihydroethidieum (DHE, red) with a nuclear counterstain (DAPI, blue). DHE fluorescence for each treatment was expressed as fold change from WD with H_2O treatment (n = 8, scale bar: 200 μm). **(D–F)** C57BL/6J mice were orally administered DT-109 (0.5 mg/g body weight). At baseline (0 h), 2, 6, and 24 h, blood was collected and mononuclear cells were isolated. GSH and GSSG in mononuclear cells were analyzed using LC-MS/MS and expressed as concentrations (mmol/L) or GSH:GSSG ratio relative to baseline (n = 5). Data are presented as mean ± SEM. Statistical differences were compared using one-way ANOVA with Tukey's post hoc analysis or Kruskal-Wallis test followed by Dunn's post-hoc analysis. (For interpretation of the references to colour in this figure legend, the reader is referred to the Web version of this article.)

($p = 0.0642$). Other parameters including comorbidities, drug use and serum lipid levels were comparable between the groups. Without accounting for the above potential confounders, we found that serum glycine concentrations were significantly lower ($p<0.05$) in patients with sCAD compared to those with no sCAD (Fig. 1B). To control for potential confounding factors, we applied case-control matching and randomization and compared serum glycine concentrations in age-, sex-, and blood pressure-matched patients (Supplemental Fig. 1). Decreased glycine concentrations in serum samples from patients with sCAD remained significant when controlling for potential confounding factors ($p<0.01$, Fig. 1C). Our findings, together with previous reports indicating higher circulating glycine as a protective factor in coronary heart disease [14], led us to evaluate a causative role of glycine in atherosclerosis. To investigate a direct role of glycine in atherosclerosis, we assessed atherosclerotic plaques in the aortic sinus from *Apoe*$^{-/-}$ mice fed an amino acid (AA)-defined Western diet (WD) with or without glycine (WD_{AA} + Gly or WD_{AA} -Gly, respectively) for 10 weeks. We recently reported that *Apoe*$^{-/-}$ mice fed the WD_{AA} -Gly had increased plasma total cholesterol (TC) and hepatic steatosis without significant changes in food intake [8]. Here, we found that dietary glycine deficiency resulted in a significant increase in plaque area in the aortic sinus (by 81.8%, $p<0.05$, Fig. 1D and E). Thus, our clinical studies revealed that circulating glycine is decreased in patients with sCAD, while our mouse studies demonstrated a causative role of low glycine availability in promoting atherosclerosis.

3.2. Glycine-based treatment reduces atherosclerotic plaque size and superoxide

Considering our findings above together with previous reports [14], we reasoned that glycine-based treatment may have atheroprotective effects. By searching for glycine-based compounds with dual lipid/glucose-lowering effects, we recently identified a tripeptide of glycine combined with leucine (Gly-Gly-L-Leu, DT-109) that significantly reduced WD-induced hypercholesterolemia and hepatic steatosis in *Apoe*$^{-/-}$ mice independent of changes in food intake or body weight [8]. *Apoe*$^{-/-}$ mice were fed a WD and orally administered DT-109 (1 mg/g body weight per day) or equivalent amounts of leucine, glycine, or H_2O as control (Fig. 2A). In line with its cholesterol-lowering effects [8], we found that the expression of ATP binding cassette subfamily G member 5 (*Abcg5*) and 8 (*Abcg8*), which are known to promote hepatic-intestinal cholesterol excretion and reduce atherosclerosis [40,41], was significantly increased in livers from *Apoe*$^{-/-}$ mice treated with DT-109 (Supplemental Fig. 2). We next assessed atherosclerosis in the aortic sinus (Fig. 2B and C) and the whole aortic tree (Fig. 2D and E). While glycine administration significantly reduced the plaque area in the aortic sinus, DT-109 treatment showed the most significant atheroprotective effects and lowered the plaque area both in the aortic sinus and in the whole aortic tree (by 38.3% and 57.3%, respectively, $p<0.01$). We recently reported that glycine-based treatment protects against advanced NAFLD through induction of glutathione biosynthetic pathways and antioxidant defense in the liver [8]. Accordingly, analyses of hepatic gene expression revealed that genes encoding for key regulators of glutathione biosynthesis and metabolism including glutathione synthetase (*Gss*), glutamate-cysteine ligase modifer subunit (*Gclm*), glutathione reductase (*Gsr*), glutathione peroxidase 3 (*Gpx3*), glutathione peroxidase 6 (*Gpx6*), and glutathione S-transferase, theta 2 (*Gstt2*) were upregulated by glycine-based treatment with the most significant effect found in *Apoe*$^{-/-}$ mice treated with DT-109 (Fig. 2F). To explore a link between glycine-based treatment, redox homeostasis and atherosclerosis, we next used dihydroethidium (DHE) to evaluate superoxide, one of the major reactive oxygen species (ROS) known to promote atherosclerosis [21,30,42], in the aortic sinus. DHE fluorescence indicated a significant reduction of superoxide in the aortic sinus of *Apoe*$^{-/-}$ mice treated with DT-109 (by 40.2%, $p<0.05$, Fig. 2G and H). Taken together, these findings indicate cholesterol-lowering and antioxidant properties of glycine-based treatment leading to reduced atherosclerosis in mice.

3.3. Glycine-based intervention reduces atherosclerosis independent of lipid-lowering effects

Considering the persistent residual risk of atherosclerotic CVD despite the common use of cholesterol-lowering drugs [22,25], we next sought to evaluate the atheroprotective potential of glycine-based treatment, independent of its previously reported lipid-lowering effects [8,17,29–32]. Therefore, we devised an experimental approach to model established atherosclerosis followed by a lipid-lowering regimen. *Apoe*$^{-/-}$ mice were fed a WD for 12 weeks and a subset of the mice were euthanized, confirming established atherosclerosis in the aortic sinus and the whole aortic tree (Supplemental Fig. 3A). After confirming atherosclerosis, the rest of the mice were switched from WD feeding to a low-fat standard diet (SD). The mice were then randomized to orally receive DT-109 at 0.5 mg/g per day [8] or equivalent amounts of leucine, glycine, or H_2O for 8 additional weeks on the SD (Fig. 3A). Changing the feeding regimen from WD to SD significantly reduced hypercholesterolemia (Plasma TC, Fig. 3B) and hypertriglyceridemia (Plasma TG, Fig. 3C) as well as body weight (Supplemental Fig. 3B) and hyperglycemia (Supplemental Fig. 3C) without any differences between mice treated with DT-109, leucine, glycine, or H_2O. Similar to WD-fed mice, *Abcg5* and *Abcg8* were upregulated in livers from mice treated with DT-109 during SD feeding. However, sterol regulatory element binding transcription factor 2 (*Srebf2*), the master regulator of cholesterol biosynthetic genes [43], was significantly upregulated as well (Supplemental Fig. 4). Analysis of atherosclerosis in the aortic sinus revealed that DT-109 treatment led to a significant reduction in the plaque area (by 32.4%, $p<0.01$, Fig. 3D and E). Furthermore, glycine and DT-109 significantly reduced the plaque area in the whole aortic tree with the most significant effect found in *Apoe*$^{-/-}$ mice treated with DT-109 (by 50.6%, $p<0.001$, Fig. 3F and G). Altogether, these results indicate that glycine-based treatment reduces atherosclerosis independent of lipid-lowering effects.

3.4. Glycine-based intervention reduces plaque superoxide and enhances glutathione formation in mononuclear cells

We next evaluated the antioxidant properties of glycine-based treatment during established atherosclerosis in the absence of lipid-lowering effects. First, we evaluated the effects of glycine-based treatment on the expression of glutathione metabolic genes in the liver. In *Apoe*$^{-/-}$ mice with established atherosclerosis that were fed the SD, DT-109 treatment significantly increased the expression of *Gstt2* and *Gstt3* (Fig. 4A). To evaluate antioxidant effects in the atherosclerotic plaque, we next assessed superoxide levels in the aortic sinus. DHE fluorescence indicated a significant reduction in superoxide in *Apoe*$^{-/-}$ mice treated with DT-109 while on the SD (by 37.5%, $p<0.01$, Fig. 4B and C). To determine the direct contribution of DT-109 to glutathione formation *in vivo* we applied targeted metabolomics and kinetics studies to measure reduced glutathione (GSH) and oxidized glutathione (GSSG) following oral administration of DT-109 to mice. Blood, hearts and aortas were collected from mice at baseline and after 2, 6 and 24 h from oral administration of DT-109 (0.5 mg/g) for analyses of GSH and GSSG using LC-MS/MS (Fig. 4D). DT-109 treatment increased GSH formation in these tissues (Fig. 4E, Supplemental Fig. 5) and resulted in a time-dependent increase in the GSH/GSSG ratio in isolated mononuclear cells (Fig. 4F). These findings indicate that the atheroprotective and antioxidant properties of glycine-based treatment are independent of lipid-lowering effect and are related to enhanced GSH availability, which is known to play a major role in atherosclerosis initiation and progression in humans and mouse models [44–47].

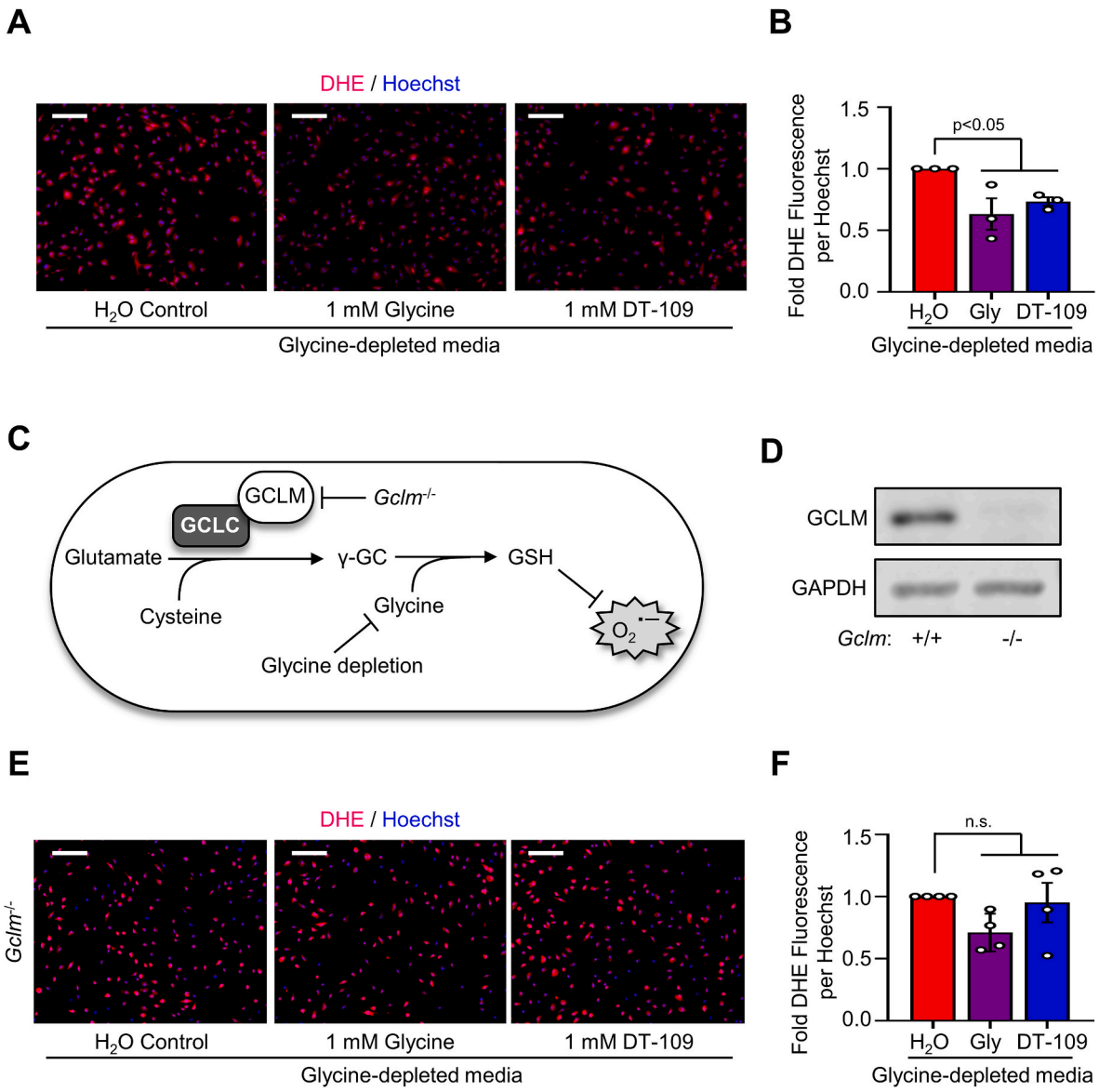

Fig. 5. Glycine-based treatment decreases superoxide generation in macrophages through GSH formation. Bone marrow-derived macrophages (BMDMs) were treated with glycine-depleted metabolic media supplemented with water control, glycine (1 mM) or DT-109 (1 mM) for 18 h. **(A)** Following treatment, BMDMs were labeled with dihydroethidium (DHE, red) for assessment of superoxide and nuclei were stained using Hoechst (blue) (scale bar: 100 μm). **(B)** DHE fluorescence was measured as mean fluorescence intensity normalized to the number of nuclei per high powered field and expressed as fold change from water control (n = 3). **(C)** Schematic diagram illustrating the production of GSH by glutamate-cysteine ligase, with the addition of inhibitors (*Gclm* KO, glycine depletion) to enhance superoxide production (γ-GC, γ-glutamylcysteine). **(D)** BMDMs were isolated from *Gclm*$^{+/+}$ and *Gclm*$^{-/-}$ mice, and the absence of GCLM was confirmed by Western blot using GAPDH as loading control (n = 3). **(E)** Following 18 h treatment with glycine-depleted media supplemented with water control, glycine (1 mM) or DT-109 (1 mM), superoxide was analyzed in BMDMs from *Gclm*$^{-/-}$ mice using DHE (scale bar: 100 μm). **(F)** DHE fluorescence was measured as mean fluorescence intensity normalized to the number of nuclei per high powered field and expressed as fold change from water control (n = 4). Data are presented as mean ± SEM showing all points. Statistical differences were compared using one-way ANOVA with Tukey's post hoc analysis or Kruskal-Wallis test followed by Dunn's post-hoc analysis. (For interpretation of the references to colour in this figure legend, the reader is referred to the Web version of this article.)

3.5. Glycine-based treatment decreases superoxide generation in macrophages through GSH

Considering our findings above in mononuclear cells together with the well-established role of monocytes and macrophages in the pathogenesis of atherosclerosis [20], we next evaluated the effects of glycine deprivation and glycine-based treatment on redox status in macrophages. In the absence of glycine or DT-109, BMDMs showed higher levels of superoxide assessed by DHE fluorescence, which was significantly reduced in BMDMs treated with 1 mM [8] of glycine or DT-109 (by 37.3%, p<0.01, or 25.9%, p<0.05, respectively, Fig. 5A and B). Loss- and gain-of-function of GSH synthesis in macrophages was shown to accelerate and inhibit atherosclerosis, respectively [46]. To determine whether the antioxidant effects of glycine-based treatment are mediated through induction of GSH formation, we next assessed superoxide in BMDMs isolated from *Gclm*$^{-/-}$ mice, in which glutathione biosynthesis is impaired [34,35,46] (Fig. 5C). We first confirmed the absence of GCLM in BMDMs isolated from *Gclm*$^{-/-}$ mice using Western blotting (Fig. 5D). Compared to BMDMs isolated from *Gclm*$^{+/+}$ mice, BMDMs from *Gclm*$^{-/-}$ mice had enhanced superoxide as visualized with DHE fluorescence (Supplemental Fig. 6); however, glycine-based treatment had no significant effects on superoxide levels in BMDMs from *Gclm*$^{-/-}$ mice (Fig. 5E and F). These experiments, combining glycine restriction and treatment with genetic inhibition of GSH formation, indicate that the

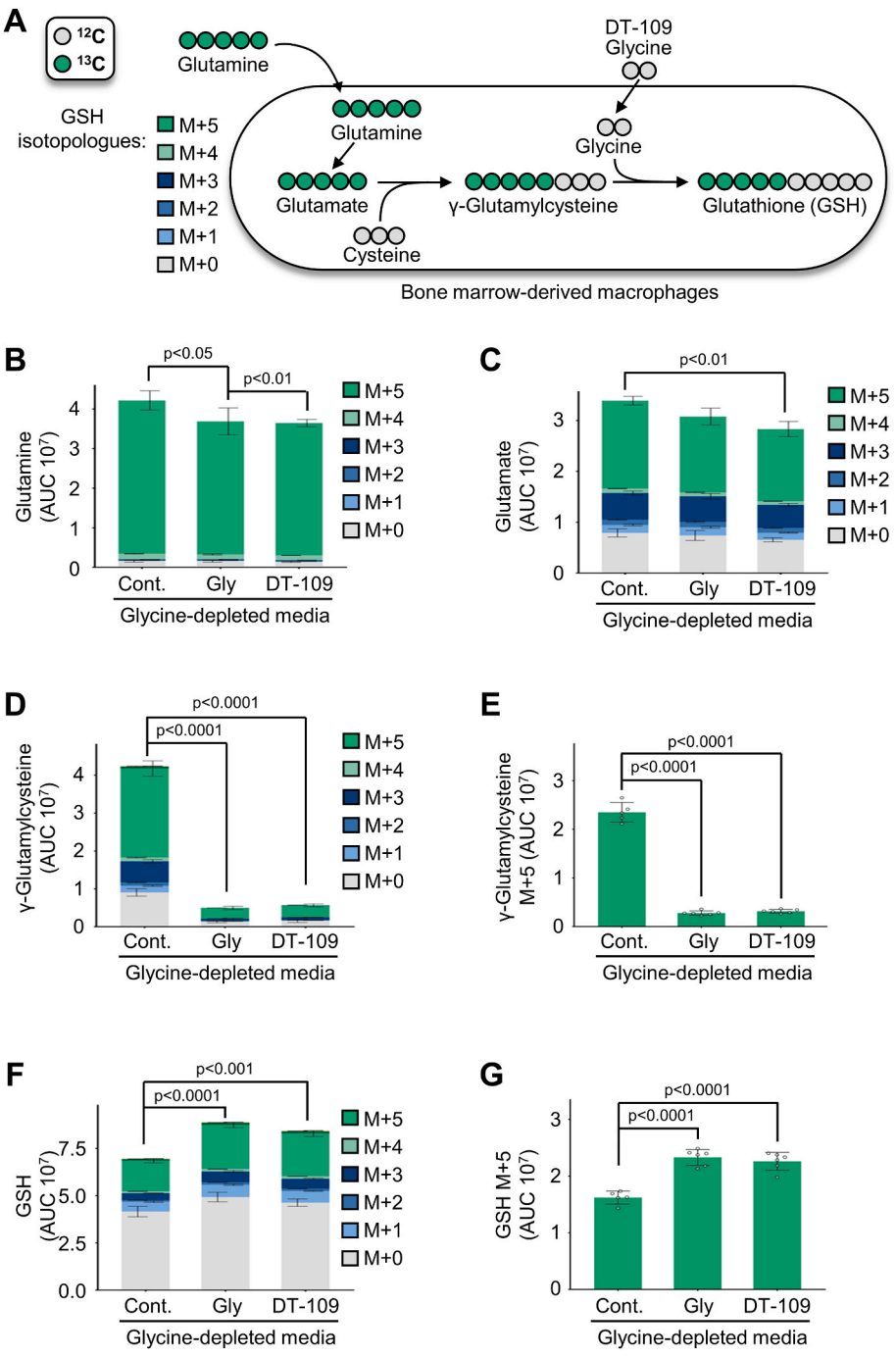

Fig. 6. Glycine-based treatment induces *de novo* GSH synthesis in macrophages. (A) Schematic representation of labeling *de novo* synthesized GSH from $^{13}C_5$-labeled glutamine in BMDMs. BMDMs were treated with glycine-depleted media for 18 h, then incubated for 5 h with glycine-depleted media supplemented with $^{13}C_5$-labeled glutamine (1 mM) and water control (cont.), glycine (Gly, 1 mM), or DT-109 (1 mM). Isotopologue distribution of indicated cellular metabolites as determined by LC-MS/MS (n = 5–6): **(B)** glutamine, **(C)** glutamate, **(D)** γ-glutamylcysteine, **(E)** M+5 isotopologue of γ-glutamylcysteine, **(F)** GSH, and **(G)** M+5 isotopologue of GSH. Metabolite peak area was normalized to total measurable ions in the sample. Data are presented as mean ± SEM. Statistical differences were compared using one-way ANOVA with Tukey's post hoc analysis.

antioxidant effects of glycine-based treatment in macrophages are mediated through induction of GSH formation.

3.6. *Glycine-based treatment induces de novo GSH synthesis in macrophages*

To determine the direct contribution of glycine-based treatment to GSH synthesis in macrophages, we next performed metabolic flux and carbon tracing studies. BMDMs were treated with $^{13}C_5$-labeled glutamine in the absence or presence of glycine or DT-109. The incorporation of $^{13}C_5$-glutamine generates a +5-mass shift (M+5) that is detected by LC-MS/MS and indicates *de novo* synthesized GSH (Fig. 6A). We first confirmed by LC-MS/MS lower glycine levels in BMDMs maintained in media without glycine or DT-109 as well as the cellular uptake of glycine and DT-109 in the treated BMDMs (Supplemental Fig. 7). Metabolites with different mass shifts due to ^{13}C incorporation are called isotopologues. The cumulative levels of all isotopologues for each metabolite were measured to determine the total relative levels in the cells. In the absence of glycine or DT-109, the precursors of GSH, glutamine (Fig. 6B), glutamate (Fig. 6C), and particularly γ-glutamylcysteine and the M+5 isotopologue of γ-glutamylcysteine (Fig. 6D and E), were accumulated. Treatment with glycine or DT-109 (1 mM) significantly decreased the accumulation of GSH precursors in BMDMs (Fig. 6B–F), indicating a block in GSH synthesis that was released upon glycine-based treatment. Accordingly, GSH was significantly increased in BMDMs treated with glycine or DT-109 (Fig. 6F), particularly the M+5 isotopologue of GSH (p<0.0001, Fig. 6G), indicating *de novo* synthesis of GSH. These findings demonstrate that glycine-based treatment induces

de novo GSH synthesis that protects macrophages from oxidant damage.

4. Discussion

Motivated by accumulating evidence linking lower circulating glycine with increased risk of CVD and related comorbidities [9–14], in the current study we evaluated 1) alterations in circulating glycine in patients with significant CAD (sCAD); 2) a causative role of glycine in atherosclerosis using dietary approaches to limit or increase glycine availability in *Apoe*$^{-/-}$ mice; 3) the therapeutic potential of glycine-based treatment (DT-109) in atherosclerosis; 4) the atheroprotective effects of glycine-based treatment independent of lipid-lowering effects; and 5) the antioxidant properties of glycine-based treatment in macrophages via induction of GSH biosynthesis through the use of genetic approaches (*Gclm*$^{-/-}$ mice) combined with targeted metabolomics, metabolic flux and carbon tracing techniques.

Including patients that underwent coronary computed tomography angiography (CCTA) to assess atherosclerosis in the coronary arteries, our clinical study revealed that circulating glycine levels are lower in patients with sCAD with or without accounting for potential confounding factors. These findings are in line with previous large-scale observational and genetic studies addressing the relationship between glycine and CVD. By studying a cohort of 4,109 participants that underwent coronary angiography, Ding et al. [13] found that circulating glycine levels are inversely associated with the risk of acute myocardial infarction after adjusting for traditional CVD risk factors. Furthermore, Wittemans et al. [14] performed genetic estimates (based on 88,800 cases with coronary heart disease and 485,266 controls) supported by observational analyses (based on 2,053 cases with coronary heart disease and 9,094 controls) and reported that low circulating glycine is associated with higher incidence of coronary heart disease. Our findings from patients with sCAD, together with the above genetic and observational studies indicating lower circulating glycine as a risk factor of CVD, led us to assess a causative role of glycine in atherosclerosis, the underlying cause of most CVDs [19].

To investigate a causative role of glycine in atherosclerosis, we applied a dietary approach to manipulate glycine availability in the *Apoe*$^{-/-}$ mouse model of atherosclerosis. We recently developed a Western diet (WD) deficient in glycine that enhanced hypercholesterolemia and hepatic steatosis in *Apoe*$^{-/-}$ mice [8]. Similarly, a recent study demonstrated that a high-fat diet deficient in glycine and its main precursor, serine, enhanced hepatic lipid accumulation in mice [31]. In line with those studies reporting enhanced hyperlipidemia and hepatic lipid accumulation due to dietary glycine restriction, we found increased atherosclerosis in *Apoe*$^{-/-}$ mice fed a glycine-deficient WD. In contrast, studies from our group and others consistently demonstrated lipid-lowering effects of dietary glycine. We previously reported that oral glycine administration lowers plasma cholesterol and triglycerides as well as hepatic steatosis in *Apoe*$^{-/-}$ mice [8,29]. Other groups similarly reported lipid-lowering effects of dietary glycine in plasma and liver using various rodent models [17,32,48]. The findings from animal studies are consistent with observational studies indicating that circulating glycine is associated with a favorable lipid profile in humans [13]. Consistent with its previously reported lipid-lowering effects, in the current study we found that oral glycine administration lowers atherosclerosis in the aortic sinus of *Apoe*$^{-/-}$ mice.

Based on consistent reports demonstrating lipid/glucose-lowering properties of glycine in humans [49,50] and animal models of cardiometabolic diseases [8,17,29,48], we recently explored glycine-based compounds that may have a therapeutic potential through a dual lipid/glucose-lowering effect. We identified DT-109 [8,51], a tripeptide composed of glycine and leucine, the two most potent glucose-lowering amino acids [52]. In addition to glycine, studies from our group and others demonstrated lipid/glucose-lowering and atheroprotective potential of leucine supplementation [53–56]. Recently, we reported that DT-109 treatment had the most potent cholesterol- and glucose-lowering effects in *Apoe*$^{-/-}$ mice on WD when compared to equivalent amounts of leucine and glycine [8]. Accordingly, in the current study, we found that DT-109 treatment had the most significant atheroprotective effects in *Apoe*$^{-/-}$ mice and lowered atherosclerosis in the whole aortic tree and the aortic sinus. These findings indicated DT-109 as a potential glycine-based treatment for atherosclerosis and warrant future evaluation of the potential additive effects of glycine and leucine [52]. Nevertheless, considering the persistent residual risk of atherosclerotic CVD despite the currently available and highly potent cholesterol-lowering drugs [22,25], it was crucial to evaluate the atheroprotective potential of DT-109 independent of its lipid/glucose-lowering properties.

To enhance the translational value of the current study, we 1) tested a lower dose of DT-109 (0.5 mg/g body weight/day) which we previously found to ameliorate advanced NAFLD in mice [8], and 2) used an experimental approach to model established atherosclerosis followed by a lipid-lowering regimen. This approach allowed us to evaluate the atheroprotective potential of DT-109, independent of its lipid/glucose-lowering properties. Indeed, we found that DT-109 treatment could not further decrease circulating cholesterol and glucose in *Apoe*$^{-/-}$ mice with established atherosclerosis that were switched from the WD to a low-fat SD. Despite the lack of lipid/glucose-lowering effects, DT-109 significantly reduced atherosclerosis in the whole aortic tree and in the aortic sinus. Furthermore, independent of lipid/glucose-lowering effects, DT-109 significantly lowered superoxide in the aortic sinus of *Apoe*$^{-/-}$ mice with established atherosclerosis, suggesting that antioxidant defense is a central mechanism by which glycine-based treatment protects against atherosclerosis.

Abnormal redox status and increased ROS are implicated in the development of many CVDs, particularly atherosclerosis [21]. Generation of superoxide, one of the major ROS, by monocytes and macrophages promotes atherosclerosis while its inhibition attenuates atherosclerosis [42,57]. The GSH-dependent antioxidant system effectively scavenges ROS, including superoxide, and plays a major role in the development of atherosclerosis [44–47,58–60]. In humans, the intima-media thickness, a marker of subclinical atherosclerosis, was inversely associated with circulating GSH [44], and a weak GSH-related antioxidant defense was found in atherosclerotic plaques [45]. Chemical and genetic inhibition of GSH synthesis increase macrophage foam-cell formation and atherosclerosis in *Apoe*$^{-/-}$ mice [46,47,60], whereas gain-of-function of glutathione synthesis in macrophages attenuates atherosclerosis [46]. Here, we found that oral administration of DT-109 induces GSH formation in blood mononuclear cells. These effects are not limited to mononuclear cells, as DT-109 enhances GSH in aortas, hearts, and liver in C57BL/6J mice [8]. In addition, our studies in isolated bone marrow-derived macrophages (BMDMs) revealed that glycine and DT-109 lower superoxide formation induced by glycine deficiency. Importantly, these effects were abolished in BMDMs from *Gclm*$^{-/-}$ mice, in which GSH formation is impaired [34,35,46], indicating that the antioxidant defense of glycine-based treatment is mediated through induction of GSH biosynthesis. Indeed, using metabolic flux and carbon tracing experiments we provide here direct evidence that glycine deficiency inhibits glutathione formation in BMDMs while glycine-based treatment induces *de novo* glutathione biosynthesis.

Our study has some limitations that may serve as future avenues of investigation. The current study expanded on our previous reports of the protective effects of DT-109 in male mice [8] and thus we evaluated the effects of DT-109 in atherosclerosis using male *Apoe*$^{-/-}$ mice. Although females tend to have a cardioprotective phenotype, studies comparing sex differences in specific aspects of atherosclerosis show females actually have greater plaque stenosis; however, males tend to have greater plaque area and inflammation leading to an increased risk of ischemic events [61]. Furthermore, previous genome-wide association studies described a variant in *CPS1* associated with enhanced circulating glycine; however, this variant is only cardioprotective in female subjects [62]. Thus, our understanding of how sex and glycine metabolism

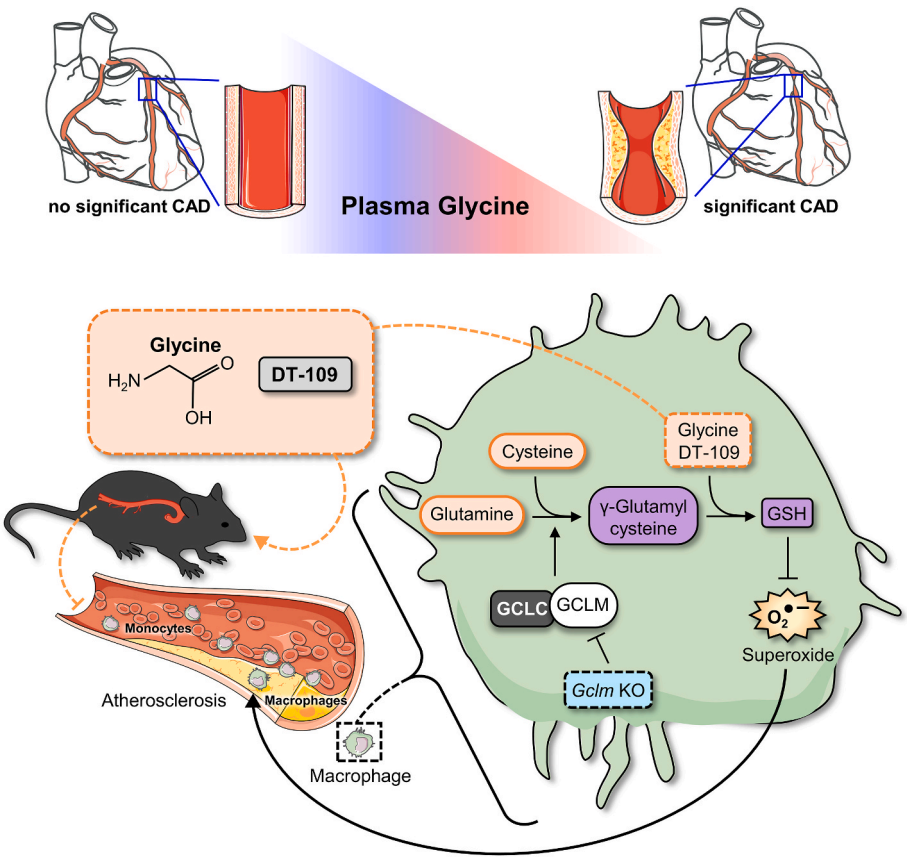

Fig. 7. Proposed model of glycine-based treatment for atherosclerosis through antioxidant effects mediated by induction of GSH biosynthesis.

influence atherosclerosis remains complex, and our findings open a new avenue of research for comparative analysis of glycine-based compounds in males and females. Our glycine-based treatment reduces atherosclerosis in mice independent of circulating lipids by enhancing the antioxidant, GSH. Previous studies demonstrated the anti-atherogenic and cardioprotective properties of antioxidant interventions [42,46,63–70]. For instance, the antioxidant Probucol reduced atheromas and plasma cholesterol in Watanabe heritable hyperlipidemic (WHHL) rabbits due to reductions in modified LDL [63,64]. Similarly, Probucol reduced cholesterol and atherosclerosis in *Apoe*$^{-/-}$ mice [65] and prevented coronary heart disease and death in SR-BI/APOE double knockout mice [66]. Analogues of Probucol that were ineffective in lowering serum cholesterol continued to reduce atherosclerosis in rabbits through reductions in LDL modification [67]. Together, using various animal models, these earlier studies highlight the contribution of antioxidant interventions in atherosclerosis independent of their effects on plasma lipid levels. Our current studies provide further evidence of the benefits of antioxidant therapeutics in atherosclerosis without targeting plasma lipids. However, our studies to date examine the contributions of DT-109 in mice, which may present a limitation due to differences in mouse models of atherosclerosis compared with humans [71]. Thus, there remains a need for exploration of DT-109 in non-mouse models of atherosclerosis, which is currently ongoing in our lab.

In summary, we report that circulating glycine levels are lower in patients with sCAD. Using dietary approaches to manipulate glycine availability in atheroprone mice, we show for the first time that glycine plays a causative role in atherosclerosis development. We further identified DT-109 as a glycine-based treatment for atherosclerosis, independent of its lipid/glucose-lowering effects, and uncovered induction of *de novo* GSH synthesis and antioxidant defense as a central mechanism of action (Fig. 7). A large body of literature including studies in humans [7,15,49,50], rodent models [8,17,29,48,72] and cellular systems [8,17,29] supports glycine-based treatments for T2D, obesity and NAFLD, well-established risk factors for atherosclerotic CVD [22,23], through lipid/glucose-lowering and antioxidant effects. Furthermore, glycine supplementation is safe and well-tolerated by humans even at high doses [73]. Considering the findings of the current study together with the above literature, the therapeutic potential of glycine-based treatment in atherosclerotic CVD warrants clinical evaluation.

Author contributions

Conception and design: O. Rom and Y.E. Chen. Acquisition, analysis or interpretation of data: O. Rom, Y. Liu, A.C. Finney, A. Ghrayeb, Y. Zhao, Y. Shukha, L. Wang, K. Rajanayake, S. Das, N.A. Rashdan, N. Weissman, L. Delgadillo, B. Wen, E. Gottlieb, and I. Mor. Resources: O. Rom, A. Yurdagul Jr., C.B. Pattillo, D. Sun, T. Hayek, E. Gottlieb, and Y. E. Chen. Drafting the manuscript: O. Rom and A.C. Finney. Critically revising the manuscript for important intellectual content: M.T. Garcia-Barrio, M. Aviram, A. Yurdagul Jr., C.B. Pattillo, C.G. Kevil, J. Zhang, D. Sun, T. Hayek, E. Gottlieb, I. Mor, and Y.E. Chen. Funding acquisition: O. Rom, J. Zhang, T. Hayek, E. Gottlieb, I. Mor, and Y.E. Chen. Supervision: O. Rom and Y.E. Chen. All authors read and approved the manuscript.

Declaration of competing interest

O. Rom, Y. Zhao, J. Zhang, and Y.E. Chen have filed a patent application based on this work (Tri-peptides and treatment of metabolic, cardiovascular, and inflammatory disorders: PCT/US2019/046052). Y. E. Chen is the founder of Diapin Therapeutics, which provided DT-109 for this study. All other authors declare that they have no competing interests.

Acknowledgements

This work was supported by the National Institutes of Health grants HL150233 (O. Rom), HL137214, HL109946, HL147527 and HL134569 (Y.E. Chen), HL145131 (A. Yurdagul Jr.), HL149264 (C G. Kevil), HL139755 (C B. Pattillo), HL138139 and HL153710 (J. Zhang), the Michigan-Israel Partnership for Research and Education (O. Rom, T. Hayek, E. Gottlieb, I. Mor, and Y.E. Chen), the American Heart Association Postdoctoral Fellowship 19POST34380224 (O. Rom), and the Israel Science Foundation 824/19 (E. Gottlieb, I. Mor, and A. Ghrayeb). We utilized services from the University of Michigan In-Vivo Animal Core supported by grant U2CDK110768 and the Animal Models and Histology Core at LSU Health Shreveport supported by grant P20GM121307 (C G. Kevil).

Appendix A. Supplementary data

Supplementary data to this article can be found online at https://doi.org/10.1016/j.redox.2022.102313.

References

[1] E. Meléndez-Hevia, P. De Paz-Lugo, A. Cornish-Bowden, M.L. Cárdenas, A weak link in metabolism: the metabolic capacity for glycine biosynthesis does not satisfy the need for collagen synthesis, J. Biosci. 34 (2009) 853–872.

[2] W. Wang, Z. Wu, Z. Dai, Y. Yang, J. Wang, G. Wu, Glycine metabolism in animals and humans: implications for nutrition and health, Amino Acids 45 (2013) 463–477.

[3] A. Alves, A. Bassot, A.L. Bulteau, L. Pirola, B. Morio, Glycine metabolism and its alterations in obesity and metabolic diseases, Nutrients 11 (2019) 1356.

[4] J. Hitzel, E. Lee, Y. Zhang, S.I. Bibli, X. Li, S. Zukunft, B. Pflüger, J. Hu, C. Schürmann, A.E. Vasconez, J.A. Oo, A. Kratzer, S. Kumar, F. Rezende, I. Josipovic, D. Thomas, H. Giral, Y. Schreiber, G. Geisslinger, C. Fork, X. Yang, F. Sigala, C.E. Romanoski, J. Kroll, H. Jo, U. Landmesser, A.J. Lusis, D. Namgaladze, I. Fleming, M.S. Leisegang, J. Zhu, R.P. Brandes, Oxidized phospholipids regulate amino acid metabolism through MTHFD2 to facilitate nucleotide release in endothelial cells, Nat. Commun. 9 (2018) 2292.

[5] D. Garcia-Santos, M. Schranzhofer, R. Bergeron, A.D. Sheftel, P. Ponka, Extracellular glycine is necessary for optimal hemoglobinization of erythroid cells, Haematologica 102 (2017) 1314–1323.

[6] J.T. Brosnan, E.P. Wijekoon, L. Warford-Woolgar, N.L. Trottier, M.E. Brosnan, J. A. Brunton, R.F. Bertolo, Creatine synthesis is a major metabolic process in neonatal piglets and has important implications for amino acid metabolism and methyl balance, J. Nutr. 139 (2009) 1292–1297.

[7] A. Mardinoglu, E. Bjornson, C. Zhang, M. Klevstig, S. Söderlund, M. Ståhlman, M. Adiels, A. Hakkarainen, N. Lundbom, M. Kilicarslan, B.M. Hallström, J. Lundbom, B. Vergès, P.H.R. Barrett, G.F. Watts, M.J. Serlie, J. Nielsen, M. Uhlén, U. Smith, H.U. Marschall, M.R. Taskinen, J. Boren, Personal model-assisted identification of NAD+ and glutathione metabolism as intervention target in NAFLD, Mol. Syst. Biol. 13 (2017) 916.

[8] O. Rom, Y. Liu, Z. Liu, Y. Zhao, J. Wu, A. Ghrayeb, L. Villacorta, Y. Fan, L. Chang, L. Wang, C. Liu, D. Yang, J. Song, J.C. Rech, Y. Guo, H. Wang, G. Zhao, W. Liang, Y. Koike, H. Lu, T. Koike, T. Hayek, S. Pennathur, C. Xi, B. Wen, D. Sun, M. T. Garcia-Barrio, M. Aviram, E. Gottlieb, I. Mor, W. Liu, J. Zhang, Y.E. Chen, Glycine-based treatment ameliorates NAFLD by modulating fatty acid oxidation, glutathione synthesis, and the gut microbiome, Sci. Transl. Med. 12 (2020), eaaz2841.

[9] C.B. Newgard, J. An, J.R. Bain, M.J. Muehlbauer, R.D. Stevens, L.F. Lien, A. M. Haqq, S.H. Shah, M. Arlotto, C.A. Slentz, J. Rochon, D. Gallup, O. Ilkayeva, B. R. Wenner, W.S. Yancy Jr., H. Eisenson, G. Musante, R.S. Surwit, D.S. Millington, M.D. Butler, L.P. Svetkey, A branched-chain amino acid-related metabolic signature that differentiates obese and lean humans and contributes to insulin resistance, Cell Metabol. 9 (2009) 311–326.

[10] M. Guasch-Ferré, A. Hruby, E. Toledo, C.B. Clish, M.A. Martínez-González, J. Salas-Salvadó, F.B. Hu, Metabolomics in prediabetes and diabetes: a systematic review and metaanalysis, Diabetes Care 39 (2016) 833–846.

[11] X. Li, L. Sun, W. Zhang, H. Li, S. Wang, H. Mu, Q. Zhou, Y. Zhang, Y. Tang, Y. Wang, W. Chen, R. Yang, J. Dong, Association of serum glycine levels with metabolic syndrome in an elderly Chinese population, Nutr. Metab. 15 (2018) 89.

[12] M. Gaggini, F. Carli, C. Rosso, E. Buzzigoli, M. Marietti, V.D. Latta, D. Ciociaro, M. L. Abate, R. Gambino, M. Cassader, E. Bugianesi, A. Gastaldelli, Altered amino acid concentrations in NAFLD: impact of obesity and insulin resistance, Hepatology 67 (2018) 145–158.

[13] Y. Ding, G.F.T. Svingen, E.R. Pedersen, J.F. Gregory, P.M. Ueland, G.S. Tell, O. K. Nygård, Plasma glycine and risk of acute myocardial infarction in patients with suspected stable angina pectoris, J. Am. Heart Assoc. 5 (2015), e002621.

[14] L.B.L. Wittemans, L.A. Lotta, C. Oliver-Williams, I.D. Stewart, P. Surendran, S. Karthikeyan, F.R. Day, A. Koulman, F. Imamura, L. Zeng, J. Erdmann, H. Schunkert, K.T. Khaw, J.L. Griffin, N.G. Forouhi, R.A. Scott, A.M. Wood, S. Burgess, J.M.M. Howson, J. Danesh, N.J. Wareham, A.S. Butterworth, C. Langenberg, Assessing the causal association of glycine with risk of cardio-metabolic diseases, Nat. Commun. 10 (2019) 1060.

[15] R.V. Sekhar, S.V. McKay, S.G. Patel, A.P. Guthikonda, V.T. Reddy, A. Balasubramanyam, F. Jahoor, Glutathione synthesis is diminished in patients with uncontrolled diabetes and restored by dietary supplementation with cysteine and glycine, Diabetes Care 34 (2011) 162–167.

[16] R. Yan-Do, E. Duong, J.E. Manning Fox, X. Dai, K. Suzuki, S. Khan, A. Bautista, M. Ferdaoussi, J. Lyon, X. Wu, S. Cheley, P.E. MacDonald, M. Braun, A glycine-insulin autocrine feedback loop enhances insulin secretion from human β-cells and is impaired in type 2 diabetes, Diabetes 65 (2016) 2311–2321.

[17] S. Takashima, K. Ikejima, K. Arai, J. Yokokawa, K. Kon, S. Yamashina, S. Watanabe, Glycine prevents metabolic steatohepatitis in diabetic KK-Ay mice through modulation of hepatic innate immunity, Am. J. Physiol. Gastrointest. Liver Physiol. 311 (2016) G1105–G1113.

[18] O. Rom, L. Villacorta, J. Zhang, Y.E. Chen, M. Aviram, Emerging therapeutic potential of glycine in cardiometabolic diseases: dual benefits in lipid and glucose metabolism, Curr. Opin. Lipidol. 29 (2018) 428–432.

[19] J. Frostegård, Immunity, atherosclerosis and cardiovascular disease, BMC Med. 11 (2013) 117.

[20] K.J. Moore, F.J. Sheedy, E.A. Fisher, Macrophages in atherosclerosis: a dynamic balance, Nat. Rev. Immunol. 13 (2013) 709–721.

[21] K.K. Griendling, R.M. Touyz, J.L. Zweier, S. Dikalov, W. Chilian, Y.R. Chen, D. G. Harrison, A. Bhatnagar, American heart association council on basic cardiovascular Sciences, measurement of reactive oxygen species, reactive nitrogen species, and redox-dependent signaling in the cardiovascular system: a scientific statement from the American heart association, Circ. Res. 119 (2016) e39–75.

[22] C.W. Tsao, A.W. Aday, Z.I. Almarzooq, A. Alonso, A.Z. Beaton, M.S. Bittencourt, A. K. Boehme, A.E. Buxton, A.P. Carson, Y. Commodore-Mensah, M.S.V. Elkind, K. R. Evenson, C. Eze-Nliam, J.F. Ferguson, G. Generoso, J.E. Ho, R. Kalani, S.S. Khan, B.M. Kissela, K.L. Knutson, D.A. Levine, T.T. Lewis, J. Liu, M.S. Loop, J. Ma, M. E. Mussolino, S.D. Navaneethan, A.M. Perak, R. Poudel, M. Rezk-Hanna, G.A. Roth, E.B. Schroeder, S.H. Shah, E.L. Thacker, L.B. VanWagner, S.S. Virani, J.H. Voecks, N.Y. Wang, K. Yaffe, S.S. Martin, American heart association council on epidemiology and prevention statistics committee and stroke statistics subcommittee, heart disease and stroke statistics-2022 update: a report from the American heart association, Circulation 145 (2022) e153–e639.

[23] A. Lonardo, F. Nascimbeni, A. Mantovani, G. Targher, Hypertension, diabetes, atherosclerosis and NASH: cause or consequence? J. Hepatol. 68 (2018) 335–352.

[24] E.S. Ford, U.A. Ajani, J.B. Croft, J.A. Critchley, D.R. Labarthe, T.E. Kottke, W. H. Giles, S. Capewell, Explaining the decrease in U.S. deaths from coronary disease, 1980-2000, N. Engl. J. Med. 356 (2007) 2388–2398.

[25] R.C. Hoogeveen, C.M. Ballantyne, Residual cardiovascular risk at low LDL: remnants, lipoprotein(a), and inflammation, Clin. Chem. 67 (2021) 143–153.

[26] O. Rom, Y.E. Chen, M. Aviram, Genetic variants associated with cardiovascular diseases and related risk factors highlight novel potential therapeutic approaches, Curr. Opin. Lipidol. 32 (2021) 148–150.

[27] D.I. Swerdlow, D. Preiss, K.B. Kuchenbaecker, M.V. Holmes, J.E. Engmann, T. Shah, R. Sofat, S. Stender, P.C. Johnson, R.A. Scott, M. Leusink, N. Verweij, S. J. Sharp, Y. Guo, C. Giambartolomei, C. Chung, A. Peasey, A. Amuzu, K. Li, J. Palmen, P. Howard, J.A. Cooper, F. Drenos, Y.R. Li, G. Lowe, J. Gallacher, M. C. Stewart, I. Tzoulaki, S.G. Buxbaum, D.L. van der A, N.G. Forouhi, N.C. Onland-Moret, Y.T. van der Schouw, R.B. Schnabel, J.A. Hubacek, R. Kubinova, M. Baceviciene, A. Tamosiunas, A. Pajak, R. Topor-Madry, U. Stepaniak, S. Malyutina, D. Baldassarre, B. Sennblad, E. Tremoli, U. de Faire, F. Veglia, I. Ford, J.W. Jukema, R.G. Westendorp, G.J. de Borst, P.A. de Jong, A. Algra, W. Spiering, A.H. Maitland-van der Zee, O.H. Klungel, A. de Boer, P.A. Doevendans, C.B. Eaton, J.G. Robinson, D. Duggan, , DIAGRAM Consortium, MAGIC Consortium, InterAct Consortium, J. Kjekshus, J.R. Downs, A.M. Gotto, A.C. Keech, R. Marchioli, G. Tognoni, P.S. Sever, N.R. Poulter, D.D. Waters, T.R. Pedersen, P. Amarenco, H. Nakamura, J.J. McMurray, J.D. Lewsey, D.I. Chasman, P.M. Ridker, A. P. Maggioni, L. Tavazzi, K.K. Ray, S.R. Seshasai, J.E. Manson, J.F. Price, P. H. Whincup, R.W. Morris, D.A. Lawlor, G.D. Smith, Y. Ben-Shlomo, P.J. Schreiner, M. Fornage, D.S. Siscovick, M. Cushman, M. Kumari, N.J. Wareham, W. M. Verschuren, S. Redline, S.R. Patel, J.C. Whittaker, A. Hamsten, J.A. Delaney, C. Dale, T.R. Gaunt, A. Wong, D. Kuh, R. Hardy, S. Kathiresan, B.A. Castillo, P. van der Harst, E.J. Brunner, A. Tybjaerg-Hansen, M.G. Marmot, R.M. Krauss, M. Tsai, J. Coresh, R.C. Hoogeveen, B.M. Psaty, L.A. Lange, H. Hakonarson, F. Dudbridge, S. E. Humphries, P.J. Talmud, M. Kivimäki, N.J. Timpson, C. Langenberg, F. W. Asselbergs, M. Voevoda, M. Bobak, H. Pikhart, J.G. Wilson, A.P. Reiner, B. J. Keating, A.D. Hingorani, N. Sattar, HMG-coenzyme A reductase inhibition, type 2 diabetes, and bodyweight: evidence from genetic analysis and randomised trials, Lancet 385 (2015) 351–361.

[28] N. Chalasani, Z. Younossi, J.E. Lavine, M. Charlton, K. Cusi, M. Rinella, S. A. Harrison, E.M. Brunt, A.J. Sanyal, The diagnosis and management of nonalcoholic fatty liver disease: practice guidance from the American Association for the Study of Liver Diseases, Hepatology 67 (2018) 328–357.

[29] O. Rom, C. Grajeda-Iglesias, M. Najjar, N. Abu-Saleh, N. Volkova, D.E. Dar, T. Hayek, M. Aviram M, Atherogenicity of amino acids in the lipid-laden macrophage model system in vitro and in atherosclerotic mice: a key role for triglyceride metabolism, J. Nutr. Biochem. 45 (2017) 24–38.

[30] Y. Liu, Y. Zhao, Y. Shukha, H. Lu, L. Wang, Z. Liu, C. Liu, Y. Zhao, H. Wang, G. Zhao, W. Liang, Y. Fan, L. Chang, A. Yurdagul Jr., C.B. Pattillo, A.W. Orr, M. Aviram, B. Wen, M.T. Garcia-Barrio, J. Zhang, W. Liu, D. Sun, T. Hayek, Y. E. Chen, O. Rom, Dysregulated oxalate metabolism is a driver and therapeutic target in atherosclerosis, Cell Rep. 36 (2021) 109420.

[31] F.I. Rome, C.C. Hughey, Disrupted liver oxidative metabolism in Glycine N-Methyltransferase-Deficient mice is mitigated by dietary methionine restriction, Mol. Metabol. 101452 (2022).

[32] P.J. White, A.L. Lapworth, R.W. McGarrah, L.C. Kwee, S.B. Crown, O. Ilkayeva, J. An, M.W. Carson, B.A. Christopher, J.R. Ball, M.N. Davies, L. Kjalarsdottir, T. George, M.J. Muehlbauer, J.R. Bain, S.D. Stevens, T.R. Koves, D.M. Muoio, J. T. Brozinick, R.E. Gimeno, M.J. Brosnan, T.P. Rolph, W.E. Kraus, S.H. Shah, C. B. Newgard Cb, Muscle-liver trafficking of BCAA-derived nitrogen underlies obesity-related Glycine depletion, Cell Rep. 33 (2020) 108375.

[33] A.S. Agatston, W.R. Janowitz, F.J. Hildner, N.R. Zusmer, M. Viamonte Jr., R. Detrano, Quantification of coronary artery calcium using ultrafast computed tomography, J. Am. Coll. Cardiol. 15 (1990) 827–832.

[34] L.A. McConnachie, I. Mohar, F.N. Hudson, C.B. Ware, W.C. Ladiges, C. Fernandez, S. Chatterton-Kirchmeier, C.C. White, R.H. Pierce, T.J. Kavanagh, Glutamate cysteine ligase modifier subunit deficiency and gender as determinants of acetaminophen-induced hepatotoxicity in mice, Toxicol. Sci. 99 (2007) 628–636.

[35] S.C. Bir, X. Shen, T.J. Kavanagh, C.G. Kevil, C.B. Pattillo, Control of angiogenesis dictated by picomolar superoxide levels, Free Radic. Biol. Med. 63 (2013) 135–142.

[36] W. Xiong, X. Zhao, L. Villacorta, O. Rom, M.T. Garcia-Barrio, Y. Guo, Y. Fan, T. Zhu, J. Zhang, R. Zeng, Y.E. Chen, Z. Jiang, L. Chang, Brown adipocyte-specific PPARgamma (peroxisome proliferator-activated receptor gamma) deletion impairs perivascular adipose tissue development and enhances atherosclerosis in mice, Arterioscler. Thromb. Vasc. Biol. 38 (2018) 1738–1747.

[37] A. Daugherty, A.R. Tall, M.J.A.P. Daemen, E. Falk, E.A. Fisher, G. García-Cardeña, A.J. Lusis, A.P. Owens 3rd, M.E. Rosenfeld, R. Virmani, American heart association council on arteriosclerosis, thrombosis and vascular biology; and council on basic cardiovascular Sciences, recommendation on design, execution, and reporting of animal atherosclerosis studies: a scientific statement from the American heart association, Circ. Res. 121 (2017) e53–e79.

[38] L. Villacorta, L. Minarrieta, S.R. Salvatore, N.K. Khoo, O. Rom, Z. Gao, R. C. Berman, S. Jobbagy, L. Li, S.R. Woodcock, Y.E. Chen, B.A. Freeman, A. M. Ferreira, F.J. Schopfer, D.A. Vitturi, In situ generation, metabolism and immunomodulatory signaling actions of nitro-conjugated linoleic acid in a murine model of inflammation, Redox Biol. 15 (2018) 522–531.

[39] A.C. Finney, S.D. Funk, J.M. Green, A. Yurdagul Jr., M.A. Rana, R. Pistorius, M. Henry, A. Yurochko, C.B. Pattillo, J.G. Traylor, J. Chen, M.D. Woolard, C. G. Kevil, A.W. Orr, EphA2 expression regulates inflammation and fibroproliferative remodeling in atherosclerosis, Circulation 8 (2017) 566–582.

[40] L. Yu, J. Li-Hawkins, R.E. Hammer, K.E. Berge, J.D. Horton, J.C. Cohen, H. H. Hobbs, Overexpression of ABCG5 and ABCG8 promotes biliary cholesterol secretion and reduces fractional absorption of dietary cholesterol, J. Clin. Invest. 110 (2002) 671–680.

[41] F. Basso, L.A. Freeman, C. Ko, C. Joyce, M.J. Amar, R.D. Shamburek, T. Tansey, F. Thomas, J. Wu, B. Paigen, A.T. Remaley, S. Santamarina-Fojo, H.B. Brewer Jr., Hepatic ABCG5/G8 overexpression reduces apoB-lipoproteins and atherosclerosis when cholesterol absorption is inhibited, J. Lipid Res. 48 (2007) 114–126.

[42] A.E. Vendrov, Z.S. Hakim, N.R. Madamanchi, M. Rojas, C. Madamanchi, M. S. Runge, Atherosclerosis is attenuated by limiting superoxide generation in both macrophages and vessel wall cells, Arterioscler. Thromb. Vasc. Biol. 27 (2007) 2714–2721.

[43] J.D. Horton, J.L. Goldstein, M.S. Brown, SREBPs: activators of the complete program of cholesterol and fatty acid synthesis in the liver, J. Clin. Invest. 109 (2002) 1125–1131.

[44] R. Schutte, A.E. Schutte, H.W. Huisman, J.M. van Rooyen, N.T. Malan, S. Péter, C. M. Fourie, F.H. van der Westhuizen, R. Louw, C.A. Botha, L. Malan, Blood glutathione and subclinical atherosclerosis in African men: the SABPA Study, Am. J. Hypertens. 22 (2009) 1154–1159.

[45] D. Lapenna, S. de Gioia, G. Ciofani, A. Mezzetti, S. Ucchino, A.M. Calafiore, A. M. Napolitano, C. Di Ilio, F. Cuccurullo F, Glutathione-related antioxidant defenses in human atherosclerotic plaques, Circulation 97 (1998) 1930–1934.

[46] A. Callegari, Y. Liu, C.C. White, A. Chait, P. Gough, E.W. Raines, D. Cox, T. J. Kavanagh, M.E. Rosenfeld, Gain and loss of function for glutathione synthesis: impact on advanced atherosclerosis in apolipoprotein E deficient mice, Arterioscler. Thromb. Vasc. Biol. 31 (2011) 2473–2482.

[47] M. Torzewski, V. Ochsenhirt, A.L. Kleschyov, M. Oelze, A. Daiber, H. Li, H. Rossmann, S. Tsimikas, K. Reifenberg, F. Cheng, H.A. Lehr, S. Blankenberg, U. Förstermann, T. Münzel, K.J. Lackner, Deficiency of glutathione peroxidase-1 accelerates the progression of atherosclerosis in apolipoprotein E-deficient mice, Arterioscler. Thromb. Vasc. Biol. 27 (2007) 850–857.

[48] M. El Hafidi, I. Pérez, J. Zamora, V. Soto, G. Carvajal-Sandoval, G. Baños G, Glycine intake decreases plasma free fatty acids, adipose cell size, and blood pressure in sucrose-fed rats, Am. J. Physiol. Regul. Integr. Comp. Physiol. 287 (2004) R1387–R1393.

[49] M.C. Gannon, J.A. Nuttall, F.Q. Nuttall, The metabolic response to ingested glycine, Am. J. Clin. Nutr. 76 (2002) 1302–1307.

[50] M. Cruz, C. Maldonado-Bernal, R. Mondragón-Gonzalez, R. Sanchez-Barrera, N. H. Wacher, G. Carvajal-Sandoval, J. Kumate, Glycine treatment decreases proinflammatory cytokines and increases interferon-γ in patients with type 2 diabetes, J. Endocrinol. Invest. 31 (2008) 694–699.

[51] J. Zhang, C. Xue, T. Zhu, A. Vivekanandan, S. Pennathur, Z.A. Ma, Y.E. Chen, A tripeptide Diapin effectively lowers blood glucose levels in male type 2 diabetes mice by increasing blood levels of insulin and GLP-1, PLoS One 8 (2013), e83509.

[52] J.F. Iverson, M.C. Gannon, F.Q. Nuttall, Interaction of ingested leucine with glycine on insulin and glucose concentrations, J. Amino Acids (2014) 521941.

[53] Y. Macotela, B. Emanuelli, A.M. Bång, D.O. Espinoza, J. Boucher, K. Beebe, W. Gall, C.R. Kahn, Dietary leucine - an environmental modifier of insulin resistance acting on multiple levels of metabolism, PLoS One 6 (2011), e21187.

[54] Y. Zhao, X.Y. Dai, Z. Zhou, G.X. Zhao, X. Wang, M.J. Xu, Leucine supplementation via drinking water reduces atherosclerotic lesions in apoE null mice, Acta Pharmacol. Sin. 37 (2016) 196–203.

[55] C. Grajeda-Iglesias, O. Rom, S. Hamoud, N. Volkova, T. Hayek, N. Abu-Saleh, M. Aviram, Leucine supplementation attenuates macrophage foam-cell formation: studies in humans, mice, and cultured macrophages, Biofactors 44 (2018) 245–262.

[56] C. Grajeda-Iglesias, O. Rom, M. Aviram, Branched-chain amino acids and atherosclerosis: friends or foes? Curr. Opin. Lipidol. 29 (2018) 166–169.

[57] M.K. Cathcart, Regulation of superoxide anion production by NADPH oxidase in monocytes/macrophages: contributions to atherosclerosis, Arterioscler. Thromb. Vasc. Biol. 24 (2004) 23–28.

[58] C.C. Winterbourn, Revisiting the reactions of superoxide with glutathione and other thiols, Arch. Biochem. Biophys. 595 (2016) 68–71.

[59] K. Aquilano, S. Baldelli, M.R. Ciriolo, Glutathione: new roles in redox signaling for an old antioxidant, Front. Pharmacol. 5 (2014) 196.

[60] X. Yang, H. Yao, Y. Chen, L. Sun, Y. Li, X. Ma, S. Duan, X. Li, R. Xiang, J. Han, Y. Duan, Inhibition of glutathione production induces macrophage CD36 expression and enhances cellular-oxidized low density lipoprotein (oxLDL) uptake, J. Biol. Chem. 290 (2015) 21788–21799.

[61] J.J. Man, J.A. Beckman, I.Z. Jaffe, Sex as a biological variable in atherosclerosis, Circ. Res. 126 (2020) 1297–1319.

[62] J.A. Hartiala, W.H. Wilson Tang, Z. Wang, A.L. Crow, A.F.R. Steward, R. Robers, R. McPherson, J. Erdmann, C. Willenborg, S.L. Hazen, H. Allayee, Genome-wide association study and targeted metabolomics identifies sex-specific association of CPS1 with coronary artery disease, Nat. Commun. 7 (2016) 10558.

[63] T. Kita, Y. Nagano, M. Yokode, K. Ishii, N. Kume, A. Ooshima, H. Yoshida, C. Kawai, Probucol prevents the progression of atherosclerosis in Watanabe heritable hyperlipidemic rabbit, an animal model for familial hypercholesterolemia, Proc. Natl. Acad. Sci. U. S. A 84 (1987) 5928–5931.

[64] T.E. Carew, D.C. Schwenke, D. Steinberg, Antiatherogenic effect of probucol unrelated to its hypocholesterolemic effect: evidence that antioxidants *in vivo* can selectively inhibit low density lipoprotein degradation in macrophage-rich fatty streaks and slow the progression of atherosclerosis in the Watanabe heritable hyperlipidemic rabbit, Proc. Natl. Acad. Sci. U. S. A 84 (1987) 7725–7729.

[65] P.K. Witting, K. Pettersson, J. Letters, R. Stocker, Site-specific antiatherogenic effect of probucol in apolipoprotein E-deficient mice, Arterioscler. Thromb. Vasc. Biol. 20 (2000) E26–E33.

[66] A. Braun, S. Zhang, H.E. Miettinen, S. Ebrahim, T.M. Holm, E. Vasile, M.J. Post, D. M. Yoerger, M.H. Picard, J.L. Krieger, N.C. Andrews, M. Simons, M. Krieger, Probucol prevents early coronary heart disease and death in the high-density lipoprotein receptor SR-BI/apolipoprotein E double knockout mouse, Proc. Natl. Acad. Sci. U. S. A 12 (2003) 7283–7288.

[67] S.J. Mao, M.T. Yates, A.E. Rechtin, R.L. Jackson, W.A. Van Sickle, Antioxidant activity of probucol and its analogues in hypercholesterolemic Watanabe rabbits, J. Med. Chem. 34 (1991) 298–302.

[68] O. Rom, M. Aviram, Endogenous or exogenous antioxidants vs. pro-oxidants in macrophage atherogenicity, Curr. Opin. Lipidol. 27 (2016) 204–206.

[69] O. Rom, H. Korach-Rechtman, T. Hayek, Y. Danin-Poleg, H. Bar, Y. Kashi, M. Aviram, Acrolein increases macrophage atherogenicity in association with gut microbiota remodeling in atherosclerotic mice: protective role for the polyphenol-rich pomegranate juice, Arch. Toxicol. 91 (2017) 1709–1725.

[70] O. Rom, N. Volkova, H. Jeries, C. Grajeda-Iglesias, M. Aviram, Exogenous (pomegranate juice) or endogenous (Paraoxonase1) antioxidants decrease triacylglycerol accumulation in mouse cardiovascular disease-related tissues, Lipids 53 (2018) 1031–1041.

[71] T. Hampton, How useful are mouse models for understanding human atherosclerosis? Circulation 135 (2017) 1757–1758.

[72] M.K. Caldow, D.J. Ham, D.P. Godeassi, A. Chee, G.S. Lynch, R. Koopman, Glycine supplementation during calorie restriction accelerates fat loss and protects against further muscle loss in obese mice, Clin. Nutr. 35 (2016) 1118–1126.

[73] U. Heresco-Levy, D.C. Javitt, M. Ermilov, C. Mordel, G. Silipo, M. Lichtenstein, Efficacy of high-dose glycine in the treatment of enduring negative symptoms of schizophrenia, Arch. Gen. Psychiatr. 56 (1999) 29–36.